




Inter-Annual Variability and Trends of Sea Level and Sea Surface Temperature in the Mediterranean Sea over the Last 25 Years

BAYOUMY MOHAMED,¹  ABDALLAH MOHAMED ABDALLAH,¹ KHALED ALAM EL-DIN,¹ HAZEM NAGY,^{1,2} and MOHAMED SHALTOU^{1,3}

Abstract—Sea level and sea surface temperature inter-annual variability and trends in the Mediterranean Sea were investigated during the period 1993–2017. These were carried out using gridded absolute dynamic topography from satellite altimetry, tide gauge (TG) time series from 25 stations and gridded sea surface temperature (SST) from advanced very-high-resolution radiometer (AVHRR) data. The coastal TG data were used to verify the satellite derived sea level. Moreover, the contributions of atmospheric pressure and North Atlantic Oscillation (NAO) to sea level changes were also examined. The results revealed that the Mediterranean Sea exhibits inter-annual spatiotemporal coherent variability in both sea level and SST. The spatial variability in sea level is more significant over the Adriatic and Aegean Seas, most of the Levantine basin, and along the Tunisian shelf. Marked spatial variability in SST occurs over the central part of the Mediterranean Sea with maximum amplitude in the Tyrrhenian Sea. The highest temporal variability of sea level and SST was found in 2010 and 2003, respectively. The inter-annual variability of sea level and SST accounts for about 32% and 3% of the total variance of sea level and SST, respectively. An analysis of sea level anomaly revealed large negative values during the extended winter of 2011–2012, which may be attributed to the strong positive phase of NAO index. Satellite altimetry indicated a significant positive sea level trend of 2.7 ± 0.41 mm/year together with a significant warming of 0.036 ± 0.003 °C/year over the whole Mediterranean Sea for the period 1993–2017.

Key words: Mediterranean Sea, absolute dynamic topography, tide gauges, AVHRR, spatiotemporal variability and trends.

1. Introduction

Sea-level rise (SLR) is a key indicator of global climate change as a natural integrator for various effects. According to the Fifth Assessment Report (AR5) of the Intergovernmental Panel on Climate Change (IPCC), the Mediterranean Sea is potentially one of the most vulnerable regions to the effects of SLR due to climate change (Church et al. 2013). The Mediterranean Sea is characterized by low-lying coasts, which are exceptionally vulnerable to the impacts of an SLR of 1 m (e.g. Nile River Delta, Egypt; Dasgupta et al. 2011). Local/regional SLR differ significantly from global mean rates (Stammer et al. 2013). Therefore, regional assessments are needed for risk management, adaptation planning, and integrated coastal zone management. Recent studies demonstrate an increase in global mean sea level (GMSL) of 3.2 ± 0.4 mm/year from altimetric data and 2.8 ± 0.8 mm/year from TG data, during the period 1993–2009, after removing the influence of glacial isostatic adjustment (GIA) (Church and White 2011). Chambers et al. (2017) using altimetric data showed that during the period 1993–2015, the GMSL has risen by 3.19 ± 0.63 mm/year.

Previous studies demonstrated the relationship between sea level and SST in the Mediterranean. For example, Cazenave et al. (2001, 2002) showed that sea level in the Mediterranean Sea rose continuously almost everywhere during the period 1993–1999, except in the Ionian Sea where a sea level drop was observed. The observed SLR was strongly correlated with sea surface warming during the same period. During the period 1992–2000, fast SLR was observed in the eastern Mediterranean Sea (Fenoglio-Marc

¹ Faculty of Science, Department of Oceanography, University of Alexandria, Alexandria, Egypt. E-mail: bayomi.mabrouk@alexu.edu.eg

² Marine Institute, Oranmore, Galway, Ireland.

³ Department of Earth Sciences, University of Gothenburg, Gothenburg, Sweden.

2002) and was linked to changes in the observed SST. Vigo et al. (2005) reported a significant abrupt change in the trend of sea level anomaly (SLA) in mid-1999, which was confirmed by independent TG data. Before mid-1999, a good spatial correlation between the SLA and SST trend maps was observed, while after that time the correlation practically disappeared.

During the last few decades, altimetry and TG data have been used in several studies to investigate the influence of the NAO on sea level variations in the Mediterranean Sea (e.g., Vigo et al. 2011; Calafat et al. 2012; Landerer and Volkov 2013; Tsimplis et al. 2013). It has been shown that the inter-annual and longer-term variability of Mediterranean sea level is strongly correlated with the NAO. The observed sea level variations are strongly anticorrelated with the monthly NAO. While the winter NAO is significantly correlated with the observed sea level. The influence of NAO increases from west to east across the Mediterranean. Sea level variations and its mass component are dominated by the winter NAO. In winter 2010, a low NAO index led to a 12-cm increase in the Mediterranean sea level (Tsimplis et al. 2013).

Recent studies used a combination of altimetry and TG data to investigate sea level variability and trends in the Mediterranean Sea. Vera et al. (2009) asserted that the Ionian sub-basin showed a negative trend during 1993–1998, followed by a rising trend until 2008 due to the relaxation of the Eastern Mediterranean Transient (EMT) and the related switch of surface Ionian layer circulation from anti-cyclonic to cyclonic during March 1998 (Gačić et al. 2010). Vigo et al. (2011) showed that during 1992–2008 the temporal trend including the quadratic acceleration of the mean sea level displays an overall increase of 2.6 cm, peaking at mid-June 2003 by 3.6 cm and then dropping 1 cm until the end of 2008. Gačić et al. (2011, 2014) investigated the influence of decadal reversals of the Ionian upper layer on thermohaline properties of the Levantine Basin, in terms of the mechanism called Adriatic-Ionian Oscillating System (BIOS). Results showed that during the Ionian anti-cyclone phase, the surface water of Levantine becomes saltier due to the weakness of the Atlantic flows. The empirical orthogonal function

analysis of the sea level revealed the out-of-phase variability of the North Ionian Gyre and the Aegean/Levantine Basins sea level.

Shaltout and Omstedt (2014) used the absolute dynamic topography from satellite altimetry data during 1993–2010. They found that Mediterranean Sea level displays a seasonally significant trend, rising by 1.2–3.6 cm/decade, and exhibits annual spatial variation from – 6 to 27 cm. The sea level variation is significantly affected by the steric effect, and sea level variation west of the Gibraltar Strait. Bonaduce et al. (2016) showed that, during the period from 1993 to 2012, the estimated mean sea level trend over the Mediterranean had a positive value of 2.44 ± 0.5 mm/year. This is the same result as for Haddad et al. (2013) obtained by performing a singular spectrum analysis with altimetry data to estimate the seasonal cycle and trends over the same period. However, changes in the local sea level were substantial and altogether different in the two studies.

In recent years, several studies have investigated the warming rates of SST in the Mediterranean Sea. Rixen et al. (2005) reported that based on in situ measurements, the average temperature of the upper 150 m layer increased by about 0.5 °C during 1980–2000, while Belkin (2009) estimated a high increase in the Mediterranean SST of 1.4 °C between 1978 and 2003. Recently, AVHRR-derived SST were investigated; Criado-Aldeanueva et al. (2008) revealed a strong rise in the satellite SST of the entire Mediterranean Sea in 1992–2005 at a rate of around 0.061 ± 0.02 °C/year. While Nykjaer (2009) showed that during the period 1985–2006 lower satellite SST warming rates of about 0.03 °C/year and 0.05 °C/year for the western and the eastern Mediterranean sub-basins occurred, respectively. Skliris et al. (2012) reported, for the period 1985–2008, a satellite-derived mean annual warming rate of about 0.037 °C/year for the entire basin, about 0.026 °C/year for the western sub-basin and about 0.042 °C/year for the eastern sub-basin. Pastor et al. (2017) observed an SST warming trend of about 0.036 °C/year for the Mediterranean Sea between 1982 and 2016.

The scope of the present work is to provide a comprehensive and up-to-date assessment of sea level changes in the Mediterranean Sea and its relation to sea surface temperature, using altimetry and tide

gauge data during the period from January 1993 to December 2017. Our analysis will assess the following issues: (1) the reliability of the mean sea level (MSL) estimated from tide gauge stations and satellite altimetry; (2) the inter-annual spatiotemporal variability and trends of sea level and sea surface temperature; and (3) the correlation between sea level and SST in the Mediterranean Sea.

2. Data and Methodology

2.1. Data Sets

The following section will present the types and the sources of the data used in this paper. These data include tide gauge, satellite altimetry, sea surface temperature and sea level pressure records. Each is described in turn below.

2.1.1 Tide Gauge Data

Monthly mean sea level data for a set of 25 TG stations, which have at least 80% completeness over the period 1993–2017, were downloaded from the Permanent Service for Mean Sea Level (PSMSL 2018, <http://www.psmsl.org/>, accessed June 2018). Our focus is on the Revised Local Reference (RLR) dataset, which is recommended for scientific purposes (Woodworth and Player 2003). The RLR dataset reduces all the records collected to a common benchmark for the analysis of time series (Holgate et al. 2013). We also extended the PSMSL record for the Alexandria station with 10 years of monthly data (2006–2015), kindly provided by Prof. El-Geziry and quality controlled by Maiyza and El-Geziry (2012). Small gaps of a few-months duration in this data were linearly interpolated, while large gaps were not included in this analysis. To remove high-frequency signals less than 1-year, we computed running averages with a 1-year window and excluded the first and last 6 months of data in each time series to avoid edge effects. Figure 3 shows the TG locations numbered from west to east along the coast according to Table 1.

2.1.2 Satellite Altimetry Data

Daily gridded ($1/8^\circ \times 1/8^\circ$) sea-level maps of Absolute Dynamic Topography (ADT) in delayed-time (reanalysis), which are more precise than near real time (NRT) products (Mertz et al. 2017), were obtained from the satellite multi-mission product of the Copernicus Marine Environment Monitoring Service (CMEMS, http://marine.copernicus.eu/services-portfolio/access-to-products/?option=com_csw&view=details&product_id=SEALEVEL_MED_PHY_L4_REP_OBSERVATIONS_008_051; accessed July 2018). This product was produced by combining data from all altimeter missions (Jason-3, Sentinel-3A, HY-2A, Saral/AltiKa, Cryosat-2, Jason-2, Jason-1, T/P, ENVISAT, GFO, ERS1) and spans the period from 1993 to 2017. Several corrections have been applied to the data, including instrumental errors (orbit error, long wavelength error), geophysical corrections [dry and wet troposphere, ionosphere and inverse barometer (IB) effect], wind effects, and tides (ocean and load tides, solid earth tide and pole tide). For more details about this product (see, Carrère and Lyard 2003; Landerer and Volkov 2013). Finally, an optimal interpolation is made merging data from all the flying satellites to compute gridded SLA (Ducet et al. 2000). The ADT is defined by adding the SLA and the synthetic mean dynamic topography (SMDT), estimated by Rio et al. (2014) over the 1993–2012 period. The product was averaged monthly to use the same temporal resolution as the tide gauge data.

2.1.3 SST and NAO Data

Daily gridded ($0.25^\circ \times 0.25^\circ$) optimum interpolation SST data were derived from the advanced very-high-resolution radiometer (AVHRR) data (version2) for the Mediterranean Sea during 1993–2017. This product was obtained from National Oceanic and Atmospheric Administration (NOAA, <http://www.ncdc.noaa.gov/oisst/data-access>, accessed May 2018). Monthly time series of the North Atlantic Oscillation (NAO) Index were extracted from the NOAA database (<http://www.cpc.noaa.gov/data/teledoc/teleindcalc.shtml>, accessed May 2018). The NOAA database has been one of the most used

Table 1

Comparison of de-seasoned monthly linear trends (mm/year) from sea level anomalies at selected tide gauge (TG), barometrically corrected tide gauge (TG + IB), and co-located altimetry gridded points (ALT)

Regions	Station name (country)	Longitude	Latitude	Record length (years)	Completeness (%)	Tide gauges trends		Altimetry trends	Comparison		GIA	
						Entire period			1993–end			1993–end
						TG	(TG)*	(TG + IB)*	(ALT)*	C	RMSE (mm)	
Western basin	1-Tarifa (Spain)	- 5.603	36.009	1943–2017	93	1.01 ± 0.13	4.11 ± 0.34	4.25 ± 0.26	2.53 ± 0.28	0.66	31	- 0.08
	2-Malaga II (Spain)	- 4.417	36.712	1992–2016	96	-	2.10 ± 0.44	1.83 ± 0.35	4.00 ± 0.30	0.61	30	- 0.13
	3-Valencia (Spain)	- 0.311	39.442	1994–2016	98	-	4.17 ± 0.49	3.84 ± 0.43	2.41 ± 0.20	0.56	22	- 0.05
	4-L'Estartit (Spain)	3.200	42.050	1990–2016	100	-	2.9 ± 0.39	2.74 ± 0.26	2.52 ± 0.23	0.82	18	0.10
	5-Sete (France)	3.699	43.398	1992–2017	83	-	3.69 ± 0.49	3.63 ± 0.36	2.65 ± 0.25	0.86	26	- 0.07
	6-Marseille (France)	5.354	43.279	1885–2017	97	1.17 ± 0.03	3.10 ± 0.34	3.20 ± 0.36	3.10 ± 0.22	0.79	27	0.06
	7-Nice (France)	7.286	43.696	1978–2017	87	2.54 ± 0.21	3.29 ± 0.59	3.03 ± 0.45	2.54 ± 0.25	0.73	25	0.04
Adriatic Sea	8-Trieste (Italy)	13.758	45.647	1875–2014	87	1.09 ± 0.04	3.44 ± 0.53	3.27 ± 0.38	3.31 ± 0.43	0.74	35	- 0.15
	9-Rovinj (Croatia)	13.628	45.083	1955–2017	99	0.81 ± 0.11	1.90 ± 0.63	1.11 ± 0.49	3.17 ± 0.34	0.71	37	- 0.12
	10-Zadar (Croatia)	15.235	44.123	1994–2014	97	-	3.00 ± 0.67	2.19 ± 0.52	3.41 ± 0.29	0.83	27	- 0.08
	11-Split Gradska Luka (Croatia)	16.442	43.507	1954–2014	100	0.94 ± 0.12	4.00 ± 0.55	3.26 ± 0.41	3.55 ± 0.27	0.88	24	- 0.06
Ionian Sea	12-Dubrovnik (Croatia)	18.063	42.658	1956–2014	99	1.37 ± 0.12	4.63 ± 0.51	3.87 ± 0.39	3.87 ± 0.25	0.88	25	- 0.04
	13-Valletta (Malta)	14.533	35.820	1993–2017	81	-	0.26 ± 0.77	0.20 ± 0.66	1.33 ± 0.47	0.77	30	0.30
	14-Preveza (Greece)	20.757	38.959	1980–2016	87	1.69 ± 0.26	4.94 ± 0.52	4.29 ± 0.45	2.83 ± 0.39	0.76	34	- 0.04
	15-Levkas (Greece)	20.712	38.835	1969–2016	85	6.20 ± 0.19	8.44 ± 0.48	7.76 ± 0.42	2.79 ± 0.27	0.70	49	- 0.02
	16-Katakolon (Greece)	21.320	37.645	1969–2016	88	2.71 ± 0.19	5.41 ± 0.50	4.46 ± 0.46	3.10 ± 0.23	0.60	41	0.07
Aegean Sea	17-Siros (Greece)	24.946	37.440	1969–2016	81	-2.15 ± 0.28	2.74 ± 0.55	2.15 ± 0.51	3.70 ± 0.36	0.81	27	0.09
	18-Khalikis North (Greece)	23.593	38.472	1990–2016	92	-	5.13 ± 0.46	4.54 ± 0.38	4.25 ± 0.33	0.76	33	- 0.05
	19-Thessaloniki (Greece)	22.935	40.633	1969–2016	89	3.74 ± 0.17	4.82 ± 0.52	4.10 ± 0.42	3.85 ± 0.33	0.85	28	- 0.17
	20-Alexandroupolis (GREECE)	25.878	40.844	1969–2016	88	1.87 ± 0.19	3.50 ± 0.57	2.97 ± 0.48	3.63 ± 0.39	0.80	32	- 0.12
	21-Khios (Greece)	26.141	38.372	1969–2015	85	3.73 ± 0.22	2.74 ± 0.75	1.93 ± 0.67	3.91 ± 0.32	0.70	40	- 0.04
Levantine basin	22-Leros (Greece)	26.848	37.130	1969–2016	82	1.24 ± 0.16	1.64 ± 0.54	1.23 ± 0.50	3.43 ± 0.31	0.70	32	0.03
	23-Antalya II (Turkey)	30.617	36.833	1985–2009	85	6.44 ± 0.45	5.65 ± 0.78	5.39 ± 0.76	3.30 ± 0.31	0.72	37	- 0.09
	24-Hadera (Israel)	34.863	32.470	1992–2012	85	-	5.70 ± 0.58	5.25 ± 0.56	3.69 ± 0.34	0.72	36	0.02
	25-Alexandria (Egypt)	29.917	31.217	1944–2015	92	1.54 ± 0.11	5.00 ± 0.41	4.63 ± 0.37	3.64 ± 0.31	0.74	34	- 0.01

Correlation coefficient (C) and RMSE between de-seasoned SLA from tide gauge and altimetry. The last column shows the glacio-isostatic adjustment (GIA) correction (mm/year) (negative values indicate subsidence). (*The GIA correction was applied to the estimated trends). Italics values show insignificant trends at 95% confidence level

sources for global SST (Reynolds et al. 2007; Marullo et al. 2014). Sea surface temperature data were used to study its inter-annual variability and trend, as well as its relationship to sea level changes in the Mediterranean Sea. Data were averaged monthly to use the same temporal resolution as the tide gauge and altimetry data. Cubic spatial interpolation has been applied for sea surface temperature to obtain a spatial resolution of $1/8^\circ \times 1/8^\circ$ as in altimetry data.

2.2. Estimation of Linear Trend

In this paper, we are interested in the de-seasoned signals of the Mediterranean sea level and the SST. Therefore, before calculating the trend, we removed the mean seasonal cycle from each dataset at each grid point, to ensure that the seasonal signal does not affect the results in case of missing observations. The mean seasonal cycle has been estimated by calculating the mean monthly values for each calendar month based on full years only, to avoid biases intrusions. The mean value of each month is then removed from all corresponding months in all years (Marcos and Tsimplis 2008). The linear trends are estimated using the least squares method. The 95% confidence interval of the regression coefficient is calculated by a standard statistical method (Emery and Thomson 1998), using the following formula:

$$\mu = \pm \sqrt{\frac{\sum_{i=1}^n (y_i - \hat{y}_i)^2}{(n-2) \sum_{i=1}^n (x_i - \bar{x})^2}} t_{\alpha/2, n-2}$$

where x_i and y_i represent the months and corresponding mean sea level or SST, \bar{x} is the average of the x_i 's, \hat{y}_i is the estimated value, n is the number of observations, and $(t_{\alpha/2, n-2})$ is the students t -distribution at 95% confidence limit ($\alpha = 0.05$). For uncorrelated measurements μ is a good estimation of the error in the linear part, but deviation from this hypothesis limits its reliability. Thus, to account for uncertainties on the regression coefficient (slope), the linear trend is given by (trend = slope $\pm \mu$). In the current study, we divide the Mediterranean Sea into five sub-basins (W. Mediterranean, Adriatic, Ionian, Aegean, and Levantine) as shown in Fig. 3. This division is based on the regional differences in the sea level variability and trends. Similar divisions have

been used for the Mediterranean Sea by Tsimplis and Rixen (2002).

For the Glacial Isostatic Adjustment (GIA) correction, we use the ICE-6G_C (VM5a) model (Peltier et al. 2015) from the PSMSL. The model provides three interrelated quantities, as follows: first, the present-day rate of change of relative sea level rise (dSea), which is used to correct tide gauges; second, the present-day rate of change of geoid height (dGeoid) used to correct altimetry; and third, the present-day rate of change of the local radius of the solid earth (radial displacement dRad). Where, $d\text{Geoid} = d\text{Rad} + d\text{Sea}$. In the Mediterranean Sea, the effect of the isostatic compensation due to GIA is on the order of ± 0.3 mm/year (Zerbini et al. 1996).

Tide gauge data are corrected for the atmospheric pressure to make it comparable to the altimetry datasets, which were originally corrected for the atmospheric pressure and wind effects. In our analysis, the effect of the high frequency response to the atmospheric pressure and wind are minimized, considering monthly averaged data. The inverse barometer (IB) effect due to the low frequency response of atmospheric pressure are subtracted from the observed sea level, using the following relationship according to Gaspar and Ponte (1997):

$$\text{IB}[\text{m}] = \frac{-[\text{SLP} - \text{SLP}_{\text{ref}}]}{\rho g}$$

where SLP is the local mean sea level pressure in Pascal extracted from the re-analysis dataset of the European Centre for Medium-Range Weather Forecasts (ECMWF) (ERA-Interim; Dee et al. 2011). SLP_{ref} is the spatial mean of SLP calculated from 1993 to 2017 over the global ocean in Pascal, ρ is the sea water density ($= 1027 \text{ kg/m}^3$), and g is the gravity acceleration ($= 9.8 \text{ m/s}^2$).

2.3. EOF Analysis

To investigate the spatial-temporal variations of sea level and SST in the Mediterranean Sea, an Empirical Orthogonal Functions (EOFs) analysis (Preisendorfer and Mobley 1988; von Storch and Zwiers 1999) was applied to the gridded monthly sea level and SST anomalies over the period 1993–2017. Prior to the EOFs computation, we first removed the

seasonal cycle and linear trends from the original (observed) time series at each grid point. Second, we normalized the de-meaned time series by dividing each point time series by its standard deviation, to avoid that a point with high variability dominates the analysis. EOFs were computed using the singular value decomposition (SVD) technique outlined by (Calafat and Gomis 2009; Skliris et al. 2012). To proceed with EOF analysis, the data matrix D was created from the set of sea level or SST maps as D (m, n), where m is the number of spatial grid points (Lon. \times Lat. = 344×128) and n is the number of months (300). By using the SVD method, the matrix D can be separated into three matrices as the form:

$$D = USV^T$$

where U is an $m \times n$ orthogonal matrix whose columns are the EOFs spatial patterns, V is an $n \times n$ orthogonal matrix whose columns are the EOFs amplitude time series, which is called the principal components (PCs), and S is an $n \times n$ diagonal matrix whose elements are the square root of the eigenvalues of the spatial covariance matrix. The output spatial vectors (EOFs) are normalized to the maximum value for each mode and the results expressed in terms of dimensionless EOFs (Fenoglio-Marc 2002; Gačić et al. 2011). A significance test based on the Monte Carlo technique (Overland and Preisendorfer 1982), known as Rule N (Preisendorfer and Mobley 1988), is applied for the selection of eigenvalues in an EOF analysis which are significant at a 95% confidence interval.

3. Results and Discussion

3.1. Relative Sea Level Linear Trends from Coastal Stations

The estimated sea level linear trends are summarized in Table 1. For the entire period, all stations show significant positive trends at 95% confidence interval, except for one station in the Aegean Sea (Siros), which manifests a significant negative trend (-2.15 ± 0.28 mm/year). Large spatial variability of the trends is found and ranges from -2.15 ± 0.28 mm/year at Siros station in the

Aegean Sea to 6.44 ± 0.45 mm/year at Antalya II station in the Levantine basin. Four stations (mainly located in the eastern Mediterranean) show trends larger than 3 mm/year.

The longest time series (more than 130 years) of Marseille (in France) and Trieste (in Italy) show trends of 1.17 ± 0.03 and 1.09 ± 0.04 mm/year, respectively, which are insignificantly different from the global mean sea level rise for the twentieth century (see Church et al. 2001). By contrast Levkas (in Greece) and Antalya II (in Turkey) show large trends of 6.20 ± 0.19 and 6.44 ± 0.45 mm/year, respectively, significantly affected by local vertical land movements. The uncertainty (μ) is very small at Marseille and Trieste, as these two stations have long records. The uncertainty of the sea level linear trend depends on the length of the time series as highlighted by Fenoglio-Marc (2002) and Tsimplis et al. (2011).

During the period (1993-end), the SLA data from tide gauges have been corrected for the IB effect, and linear trends were estimated before and after this correction (Table 1; columns 8 and 9). Twenty-four stations show positive and significant trends at 95% confidence interval, while only one station (Valletta) has an insignificant trend. The atmospheric pressure contribution to the observed sea level trends is always positive, ranging from 0 to 0.96 ± 0.13 mm/year, with an average of 0.5 ± 0.12 mm/year, and explains 12 to 36% of the observed sea level variability. The GIA rate of change at each tide gauge from the ICE-6G_C (VM5a) model is also included in the last column of Table 1 and was applied to all tide gauge stations (columns of Table 1 with superscript *).

Figure 1 shows the average monthly sea level for the different stations over the period 1993–2017. The 12-month moving averages and linear trends are also depicted. Note that at all TG stations, there were large positive SLA in winter of 2010 and 2011. This agrees with previous findings by Landerer and Volkov (2013) and Bonaduce et al. (2016) over the same period in the Mediterranean Sea. In addition, in our study we found a large negative SLA for all TG stations during the winter of 2012.

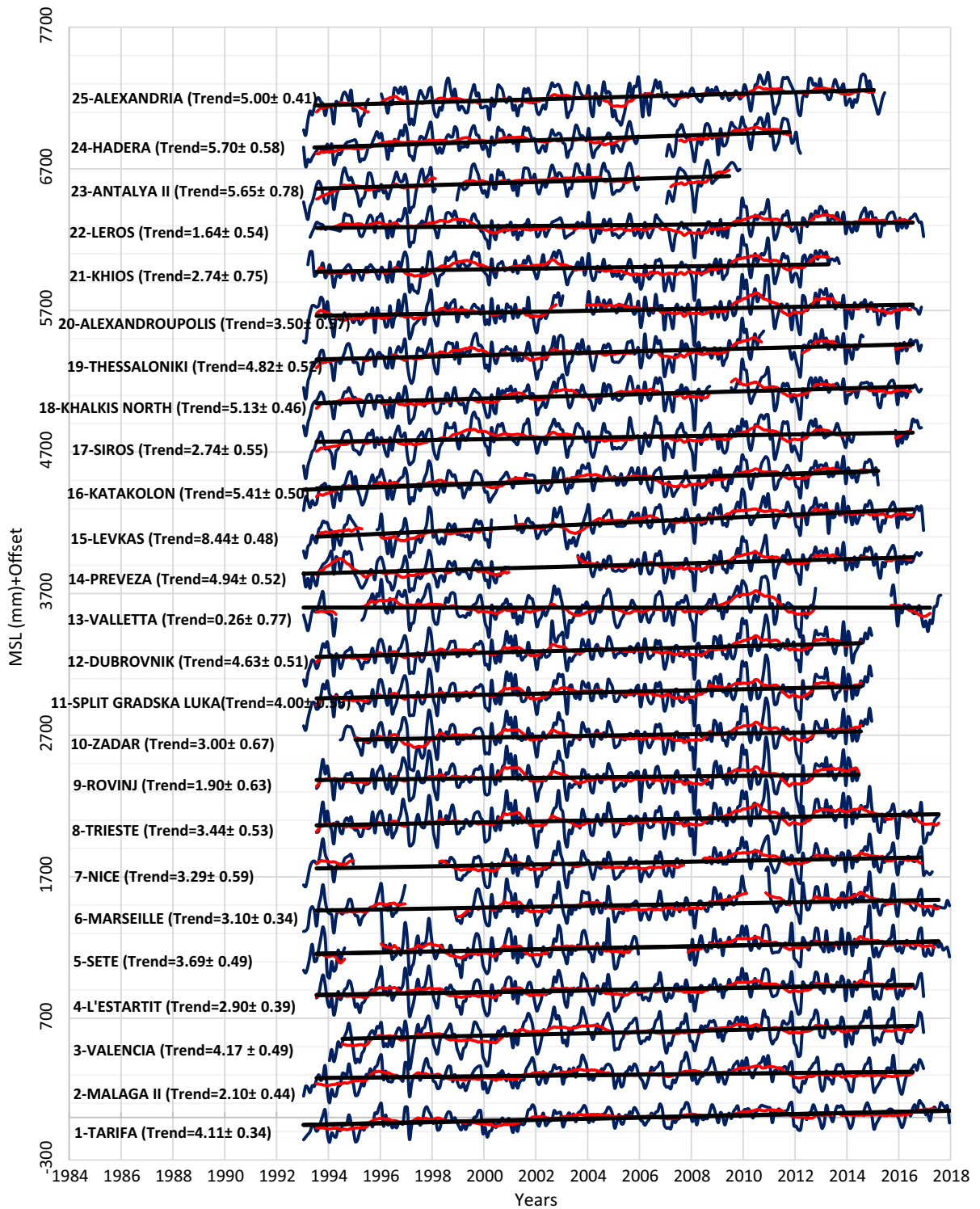


Figure 1

Monthly sea level anomaly time series at the available tide gauge stations in the Mediterranean Sea (blue). The 12-month moving averages (red) are also superimposed to clear out the data of the oscillations of periodicity less than 1 year and linear fitting (mm/year) (black) during the period 1993–2017, the GIA correction applied to the estimated trends

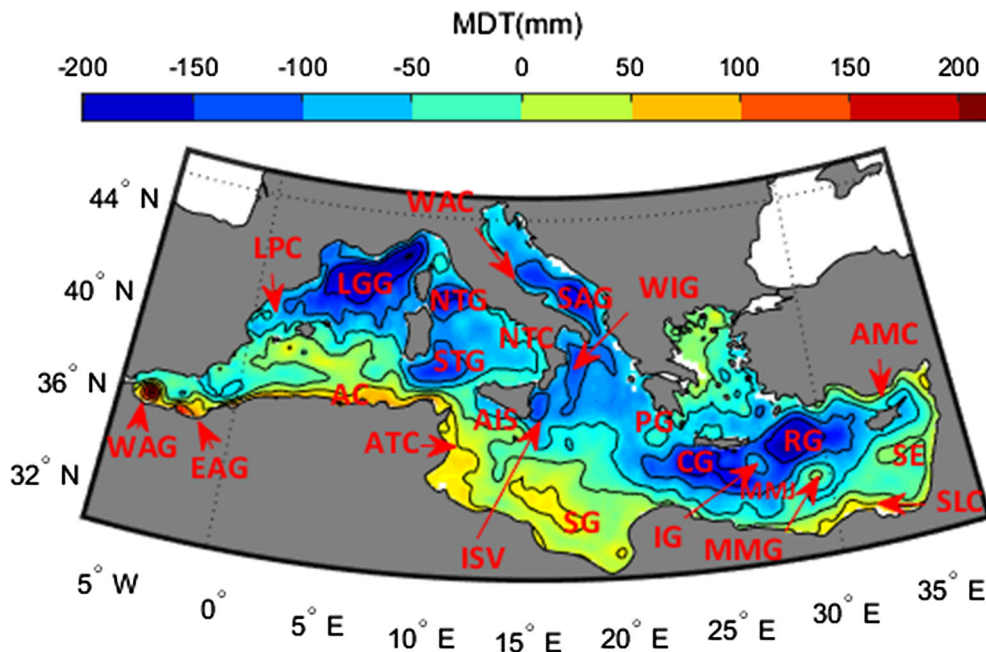


Figure 2

Main features visible on the annual Mean of Dynamic Topography (MDT) from a 25-year period (1993–2017) for the Mediterranean Sea. Names of structures and currents are listed: WAG Western Alboran Gyre, EAG Eastern Alboran Gyre, AC Algerian Current, ATC Atlantic Tunisian Current, AIS Atlantic Ionian Stream, LPC the Liguro–Provençal–Catalan Current, LGG Lions Gulf Gyre, NTC Northern Tyrrhenian Gyre, STG Southern Tyrrhenian Gyre, NTC North Tyrrhenian Current, MMJ Mid-Mediterranean Jet, SG Syrtic Gyre, WAC Western Adriatic Current, SAG Southern Adriatic Gyre, WIG Western Ionian Gyre, ISV Ionian Shelf break Vortex, PG Pelops Gyre, CG Cretan Gyre, IG Ierapetra Gyre, MMG Mersa-Matruh Gyre, SE Shikmona Eddy, RG Rhodes Gyre, SLC Southern Levantine Current, AMC Asia Minor Current

3.2. Absolute Sea Level Linear Trend Mapping from Altimetry Data

The annual Mean of Dynamic Topography (MDT) of the Mediterranean Sea has been used to describe the sea level variability and to identify areas of cyclonic/anti-cyclonic gyre systems. The area of cyclonic circulation is also used as a primary indicator of intermediate/deep water formation site, although strong cyclonic circulation areas are not automatically considered as dense water formation sites (Shaltout and Omstedt 2014).

The average Mediterranean MDT ranges from -201 to 214 mm (Fig. 2). The maximum values occurred in the Alboran sub-basin, partly indicating two Alboran anticyclonic gyres (WAG and EAG), while the minimum values occurred near the Gulf of Lions and in the Rhodes gyre, indicating two regions of cyclonic circulation (these two regions represent source of dense water formation). The average

Mediterranean MDT decreases from shallow to deep areas except in the Ionian Sea. Moreover, the average of MDT along the African coast is higher than that along the European coast, due to the Mediterranean cyclonic surface circulation. The maximum values of MDT along the European coast occurred in the Aegean Sea, probably due to the mixing with less saline water from the Black Sea (Stanev et al. 2000; Shaltout and Omstedt 2014).

Figure 2 shows that in general the Mediterranean Sea surface circulation pattern inferred by using only dynamic topography data is in good agreement with that calculated using a general circulation model and in situ measurements (Rio et al. 2007). Many interesting current patterns and eddy (cyclonic/anti-cyclonic) structures are visible on the long-term averaged of mean dynamic topography (MDT) obtained. The main Mediterranean Sea coastal currents are well marked as the Algerian Current (AC), the Liguro–Provençal–Catalan Current (LPC), North

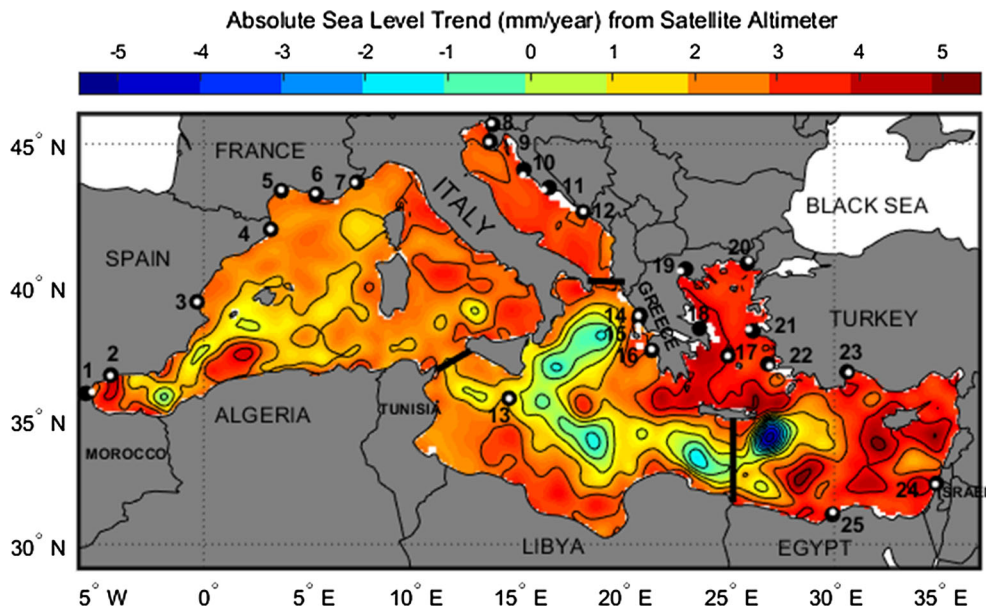


Figure 3

Map of the Mediterranean Sea level linear trends over the period (1993–2017). Seasonal signal removed, glacial-isostatic adjustment (GIA) applied. Location of the tide gauge (TG) stations used in this study (numbered black circles according to Table 1), and of the corresponding nearest altimeter grid point (white circles). The solid black line defines the separation between the different basins

Tyrrhenian Current (NTC), Southern Levantine Current (SLC), Asia Minor Current (AMC), and Western Adriatic Current (WAC). The Algerian Current (AC) moves through the Strait of Sardinia and parts into two branches, one coming into the Tyrrhenian Sea and one coming into the Ionian Sea through the Sicily strait. Where, the flow parts into two branches, the Atlantic Tunisian Current (ATC) and the Atlantic Ionian Stream (AIS) on the southern shore of Sicily. The Atlantic Ionian Stream is divided into several main branches crossing the Ionian Sea at various latitudes before joining into a unique Mid-Mediterranean Jet (MMJ). Also, strong signatures of the main Mediterranean Sea eddies are well marked. Anti-cyclonic circulation as the Western Alboran Gyre (WAG), Eastern Alboran Gyre (EAG), Pelops Gyre (PG), Ierapetra Gyre (IG), Mersa-Matruh Gyre (MMG) or Shikmona Eddy (SE) and cyclonic circulation as the Lions Gulf Gyre (LGG), Northern Tyrrhenian Gyre (NTG), Southern Tyrrhenian Gyre (STG), Cretan Gyre (CG), Rhodes Gyre (RG), Western Ionian Gyre (WIG), Ionian Shelf break Vortex (ISV), and Southern Adriatic Gyre (SAG).

The contours in Fig. 3 depict the altimetry derived sea level linear trends after the seasonal cycle and the GIA correction are removed. The GIA correction to altimetry data (dGeoid) is negative in the whole Mediterranean Sea, it ranges between -0.1 and -0.35 mm/year, with a mean value of -0.2 mm/year for the whole Basin. The absolute sea level trends show large spatial variability and gradually increases from west to east of the Mediterranean Sea. High positive trends (up to 4 mm/year) are observed over the Aegean Sea and most of the Levantine basin, particularly in areas where recurrent gyres and eddies in the circulation are found (Mersa-Matruh and Shikmona gyre). A similar peak is evident in the Ionian basin (Pelops gyre). In contrast, significant negative trends (up to -2 mm/year) are evident in the Ionian Sea, because of an important change in the circulation (EMT and BiOS effect), which has been observed in this basin since the beginning of the 1990's (Pinaridi et al. 2015; Gačić et al. 2011). We found the largest negative trend in the Levantine basin, south-east of Crete Island associated with the Ierapetra gyre (up to -5.5 mm/year).

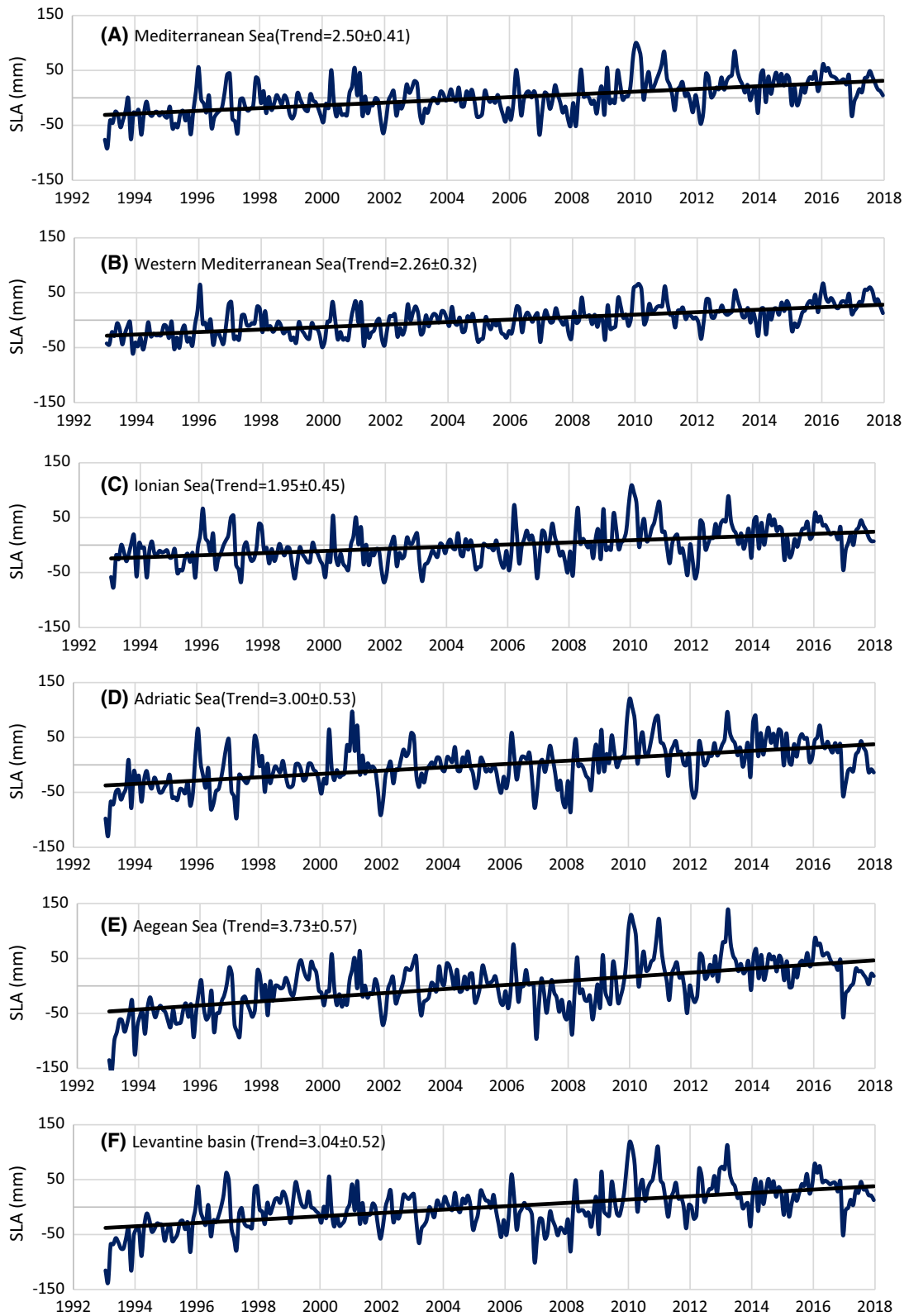


Figure 4

The de-seasoned monthly time series and linear trends (mm/year) for the averaged of SLA during the period 1993–2017, over the entire Mediterranean Sea (a), western Mediterranean (b), Ionian (c), Adriatic (d), Aegean (e), and Levantine basin (f)

Figure 4 shows the spatial mean of the de-seasoned sea level variations for the entire Mediterranean Sea and its different sub-basins as a function of time during the period from 1993 to 2017. The sea level linear trend over the whole Mediterranean Sea is about 2.5 ± 0.41 mm/year. After applying the GIA correction, the basin average trend is 2.7 ± 0.41 mm/year. While, the linear trends over the western basin, Ionian Sea, Adriatic Sea, Aegean Sea, and the Levantine basin, are about 2.26 ± 0.32 , 1.95 ± 0.45 , 3.00 ± 0.53 , 3.73 ± 0.57 , and 3.04 ± 0.52 mm/year, respectively. Note that for all the Mediterranean Sea and its different sub-basins, there were large positive SLA in winter of 2010 and 2011. This agrees with findings by Landerer and Volkov (2013) and Bonaduce et al. (2016) during the same period in the Mediterranean Sea. In addition, we found a large negative SLA during the winter of 2012 for all the Mediterranean Sea and its different sub-basins.

3.3. Comparison Between Altimetry and TG Data

In this section, the de-seasoned SLA from altimetry and tide gauge data was compared using the nearest altimeter grid points to the tide gauge stations. The results of this comparison are focused on the pattern and the correlation analysis between them. The correlations and root mean square errors (RMSEs) of the regression between the tide gauge and the nearest satellite altimeter grid point time series were chosen to measure the goodness of the fit. The lower RMSE value showed a higher similarity between high and low values of satellite altimeter and tide gauges and vice versa. In general satellite altimetry and tide gauge signals were comparable in most of the cases considered, with RMSEs that ranged between 18 and 49 mm. The two datasets were significantly correlated up to 0.88 at 95% significant level (Table 1, columns 11 and 12).

Five examples (one station from each basin) of these comparisons are plotted in Fig. 5, for the stations of Tarifa (correlation of 0.66 and RMSE 31 mm) in the western basin, Trieste (correlation of 0.74 and RMSE 35 mm) in the Adriatic Sea, Valletta (correlation of 0.77 and RMSE 30 mm) in the Ionian Sea, Siros (correlation of 0.81 and RMSE 27 mm) in the Aegean Sea, and Alexandria (correlation of 0.74 and RMSE 34 mm) in the Levantine basin. The similarity in the pattern of sea level from altimeter and tide gauge indicated good agreements between them at the most of stations in the Mediterranean Sea.

The average time-series from the 25 tide gauge stations and the average of the nearest corresponding grid points from the altimetry data have a correlation of 0.84 and RMSE of 35.27 mm. Once smoothed by a 12-month moving average, the two time-series have a correlation of 0.94 and RMSE of 8.5 mm, due to removing the seasonal cycle (Fig. 6). Sea level trends from both selected coastal tide gauge stations and altimetry data taken between 1993 and 2017 are shown in Table 1 (columns 8–10), and the results show that trends from altimetry data range from about 1.33 to 4.25 mm/year, while trends from atmospherically corrected tide gauges vary from about -0.2 to 7.76 mm/year (including GIA correction for both dataset).

3.4. Sea Level Inter-Annual Variability and Its Relation to NAO Index

Sea level signal from both altimetry and tide gauges revealed extremely large fluctuations during the extended winter months (December–March) of 2009–2010 and 2010–2011. This occurred throughout a strong negative phase of the NAO index in agreement with Landerer and Volkov (2013). The same event was observed in our study during the extended winter of 2012–2013 due to the negative phase of the NAO index. Overall, we note that from all TG stations and from altimetry data for different sub-basins (see Figs. 1, 4), there were large negative sea-level anomalies during the extended winter of 2011–2012. The low-pass-filtered (1-year moving average) of the inverted NAO index time series are overlaid in Fig. 6. The strong negative (positive) phase of NAO index event was highly correlated with

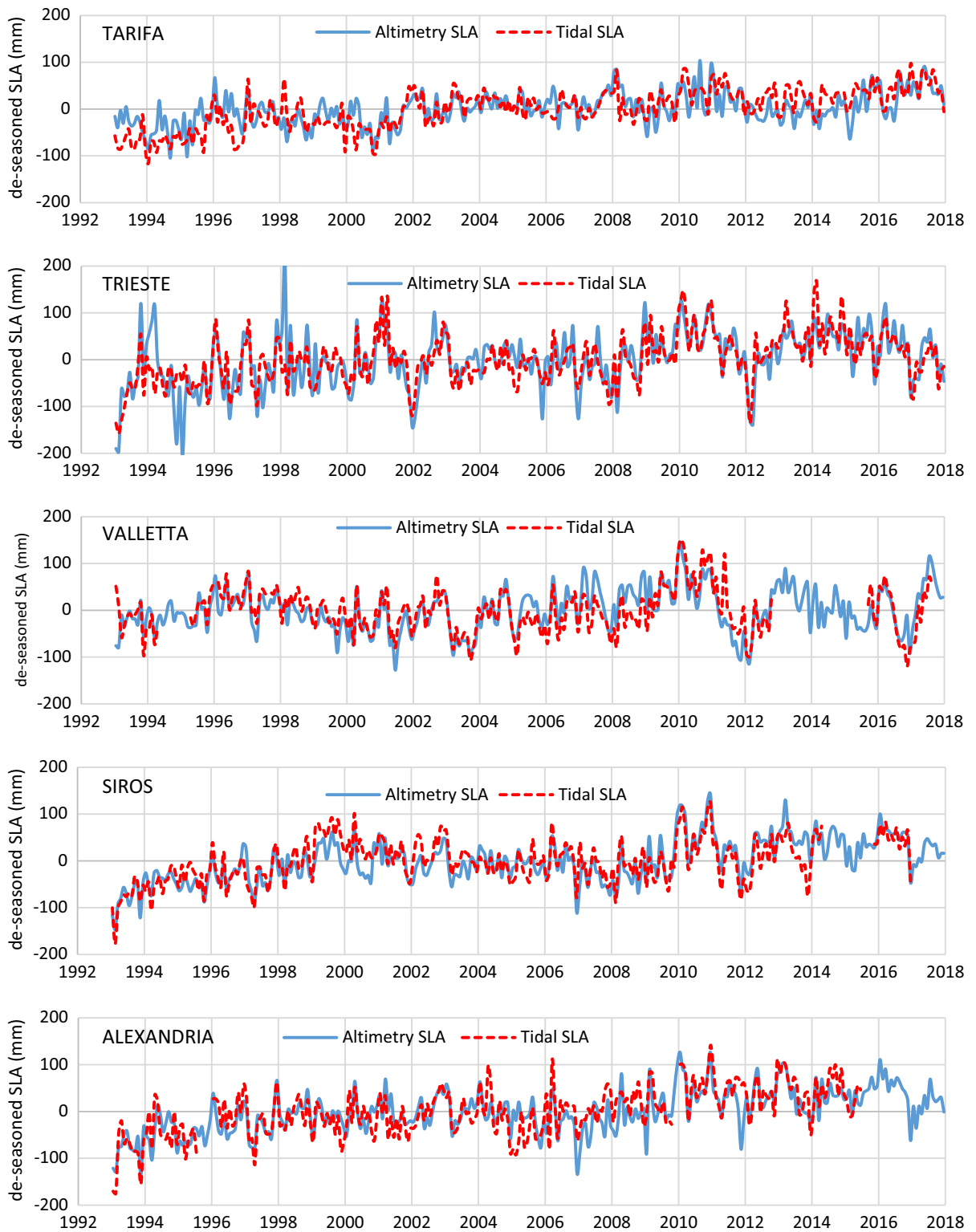


Figure 5

Comparison between de-seasoned sea level anomaly (SLA) derived from satellite altimetry and tide gauge data at selected stations (one from each basin)

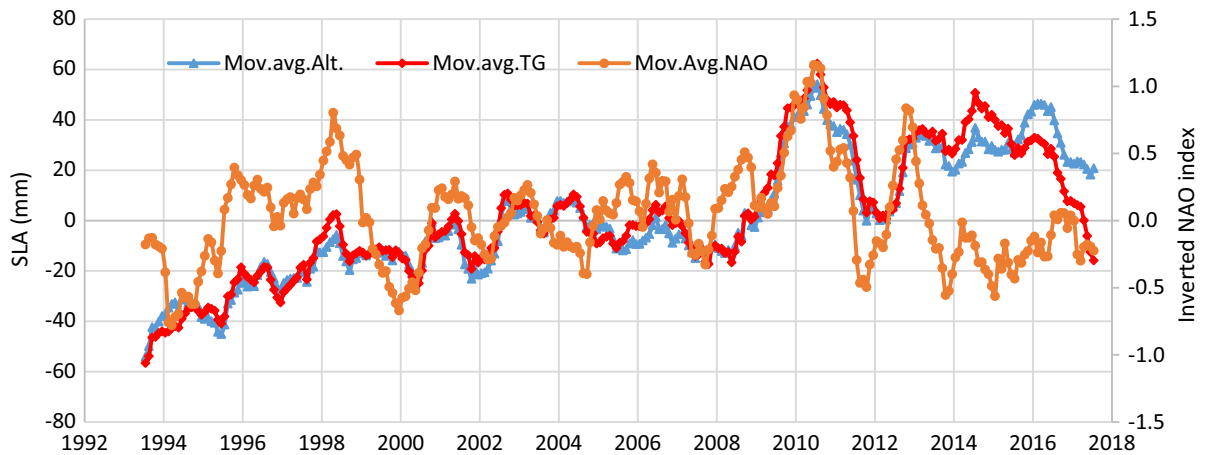


Figure 6

A 1-year running mean time series of the averaged coastal sea level from the 25 TG stations (blue) and from the altimeter nearest grid points (red), with a 1-year running mean low-pass-filtered inverted NAO index (orange) overlaid

the dramatic increase (decrease) of sea level in the Mediterranean Sea during 2010 and 2012, respectively.

As an illustration, Fig. 7 represents Mediterranean basin SLA variability over the extended winters of 2009–2010, 2010–2011, 2011–2012 and 2012–2013. These maps of SLA in the Mediterranean Sea show contrasted patterns between 2009 and 2013. During the extended winter of 2009–2010, very high positive SLA values are observed over the whole Mediterranean Sea especially in the Eastern basin and Aegean Sea. Meanwhile, during the extended winter of 2011–2012, very high negative SLA values are found, particularly in the Ionian basin.

Figure 8 compares the inverted NAO index time series with the mean deseasoned, detrended SLA during the extended wintertime only, when NAO influence is the strongest (Vigo et al. 2011). The correlation coefficient is $R = 0.59$ (statistically significant at 95% confidence level, $n = 4 \text{ months} \times 25 \text{ years} = 100$). The R -squared is 0.35, which means that after removing the seasonal signal and trend, NAO nominally explains 35% of the mean sea level variance. The correlation map between the inverted NAO index and deseasoned, detrended residual of SLA during the wintertime is shown in Fig. 9. In general, sea level is lower in NAO index positive winters, and the influence of NAO

progressively increases from west to east over the Mediterranean Sea, in agreement with (Vigo et al. 2011). The maximum correlation coefficient was observed over the Aegean Sea.

3.5. SST Linear Trends

Figure 10 depicts the variability of the temporal and spatial means of the satellite-derived SST monthly dataset over the period 1993–2017. The spatial distribution of the temporal mean shows that the average SST of Mediterranean Sea ranges from 16 to 23 °C. The maximum values occurred in the Levantine sub-basin, while the minimum values occurred near the Gulf of Lions and north of Adriatic Sea. The average SST increases eastward from Western basin to Levantine. The temporal variation of the spatial mean during the period 1993–2017, shows a clear seasonal cycle with maximum around 26 °C and minimum around 15 °C. Higher values of SST occurred during summer of 2003 (27.21 °C) and 2015 (26.81 °C) due to the exceptional heat wave in Europe during that summertime while the minimum SST were recorded during 1993 (13.92 °C) and 1996 (14.06 °C). Seasonal oscillation of SST reaches maximum at the end of August and minimum at the end of February (Criado-Aldeanueva et al. 2008).

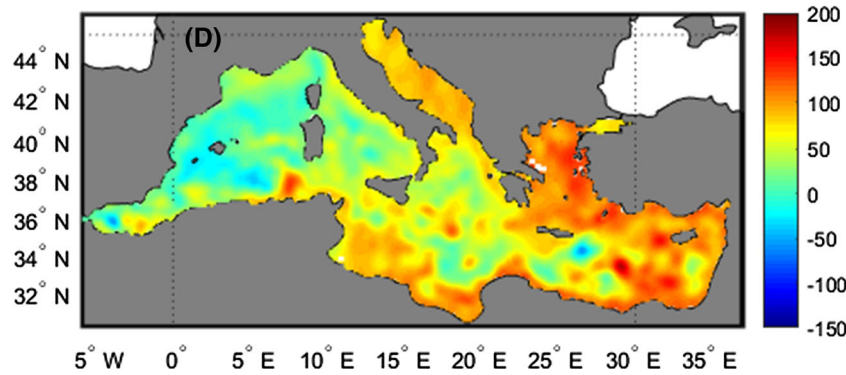
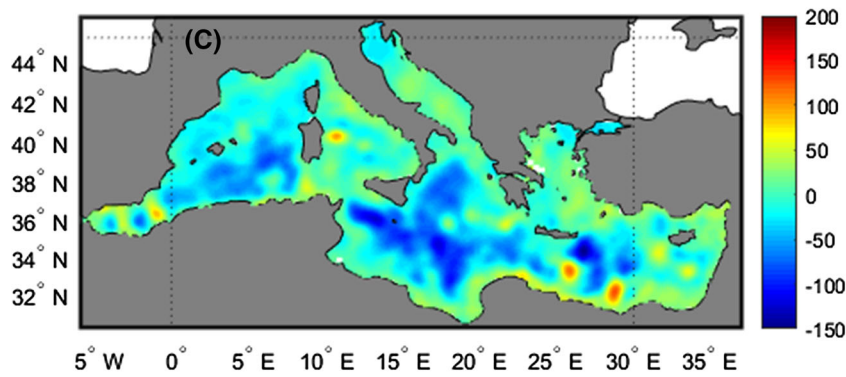
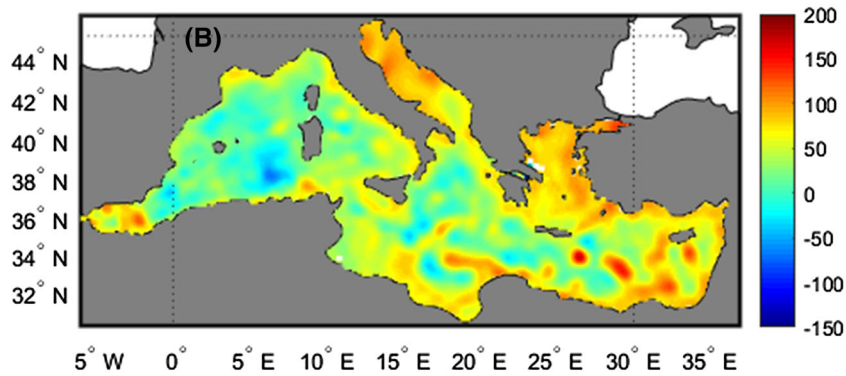
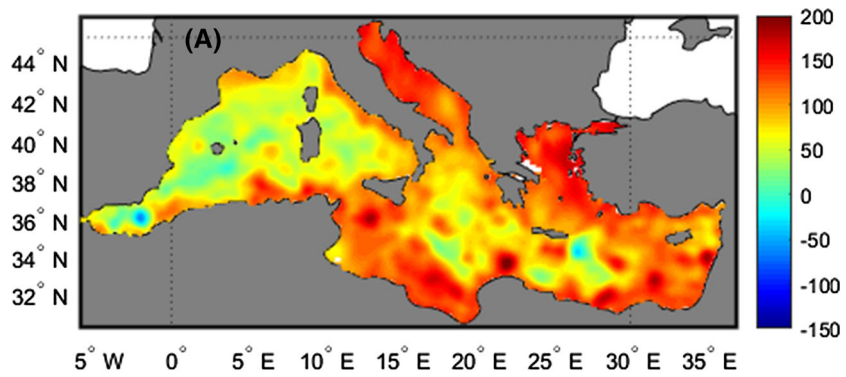


Figure 7

Maps of average SLA (mm) in Mediterranean Sea for the extended winters of **a** 2009–2010, **b** 2010–2011, **c** 2011–2012, and **d** 2012–2013

Figure 11 shows the spatial pattern of the SST linear trends over the 1993–2017 period, after the seasonal cycle was removed. The geographical distribution of the linear SST trend is like the spatial distribution observed in Fig. 3 for the linear sea level trend. The SST trend exhibits different behavior in the eastern and western sub-basins. Nonetheless, the SST trend map appears smoother everywhere than the sea level trend. A higher positive value is evident in the Levantine basin, with values up to $0.06 \text{ }^\circ\text{C/year}$ in the Cretan Arc and in the west of Cyprus, also a higher positive trend is observed in the northwest of the western basin, whereas a negative trend (up to $-0.015 \text{ }^\circ\text{C/year}$) is found in the Ionian Sea and Ierapetra gyre in the Levantine basin.

Figure 12 shows the deseasoned variation of SST for the entire Mediterranean Sea and its different sub-basins as a function of time during the period 1993–2017. The seasonality has been removed here by using the low-pass-filter of a 12-month running averages. The linear trend of SST is $0.036 \pm 0.003 \text{ }^\circ\text{C/year}$ over the whole

Mediterranean Sea, in agreement with the results of Pastor et al. (2017). While, over the western basin, Ionian Sea, Adriatic Sea, Aegean Sea, and the Levantine basin, the linear trends are 0.041 ± 0.004 , 0.030 ± 0.004 , 0.035 ± 0.005 , 0.034 ± 0.005 , $0.038 \pm 0.004 \text{ }^\circ\text{C/year}$ respectively.

3.6. EOF Analysis of the Spatiotemporal Variations of Sea Level and SST

The inter-annual variability of sea level and SST was estimated after the seasonal cycle, and the linear trend was removed from the original time series at each grid point. The spatially coherent inter-annual variability of sea level and SST was calculated using an EOF analysis. We quantified the percentage of variance represented by the seasonal cycle and the de-seasoned signal by calculating the basin-averages of temporal variances at each grid point for both the original and the residual datasets following Skliris et al. (2012). The original time series represents the total variability, whereas the residual time series represents only the deseasoned, detrended signal. We found that, on average, the inter-annual variability of sea level is responsible for 32% of the total variability in the whole basin while the inter-annual variability

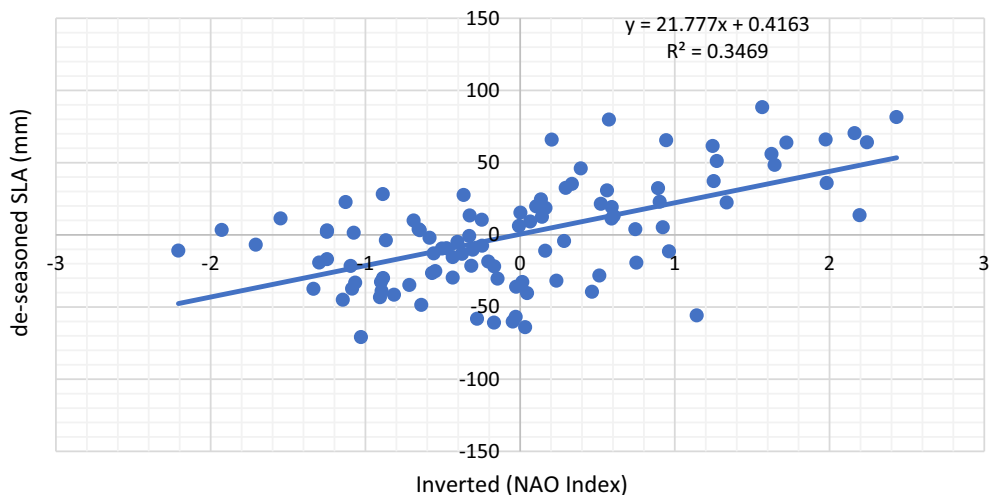


Figure 8

Scatter plot between deseasoned, detrended SLA and inverted NAO index during wintertime only (Dec–Jan–Feb–Mar)

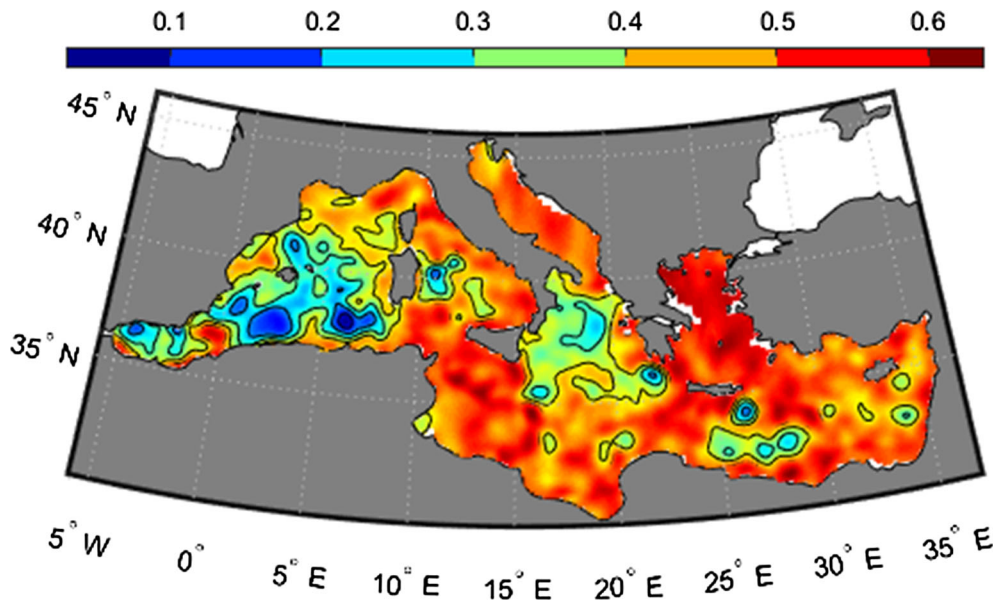


Figure 9

Pearson correlation map between the inverted NAO index and deseasoned, detrended SLA during the wintertime only (Dec–Jan–Feb–Mar)

of SST accounts for only about 3% of the total variance.

The first three EOF modes of SLA explain about 56.2% of the total deseasoned variance of the data as shown in Fig. 13. The other EOFs fail a significant test based on a Monte Carlo technique (Overland and Preisendorfer 1982). The first mode explains 44.6% of the total deseasoned variance. The spatial pattern of this mode shows an in-phase oscillation of the whole basin, i.e. an in-phase heating or cooling implying an increase or decrease of sea level of the whole Mediterranean Sea. The highest spatial variability of SLA was observed over the Adriatic and Aegean Seas, most of the Levantine basin, and along the Tunisian shelf. While the minimum spatial variability was observed in the north of Alboran Sea, south of the Balearic island, in the Ionian Sea and in the south of Crete island (Ierapetra gyre). From the corresponding PC1 time series, the highest positive peak of the inter-annual variability is encountered in 2010, and the highest negative peak was observed in winters of 2007 and 2012, which confirms the effect of NAO index and the extremely strong winter of 2012, which caused an unexpected

reversal of the North Ionian Gyre from cyclonic to anticyclonic according to Gačić et al. (2014).

The second mode of SLA explains about 7.7% of the total deseasoned variance. Its spatial distribution shows positive high value in the Ionian Sea and high negative values in the Aegean and Levantine Basins, which means the SLA has dropped in the Ionian and risen in the Levantine and Aegean Basins, and vice versa. The corresponding PC2 time series has shown prevalently decadal variability, due to the decadal inversions of the Ionian surface-layer basin-wide circulation from anticyclonic to cyclonic and vice versa (Gačić et al. 2011). The highest negative peak of inter-annual variability was encountered in 1998, due to the relaxation of the EMT and the related switch of surface Ionian layer circulation from anticyclonic to cyclonic during March 1998 (Vera et al. 2009). In general, during the Ionian anticyclonic circulation period (before 1998 and between 2006–2010). The sea level in the Levantine and Aegean basins was decreased due to the Mid-Ionian Jet was weakened by the Ionian anticyclonic circulation. Conversely, during the Ionian cyclonic period (between 1998 and 2005) the sea level in the Levantine and Aegean basins was increased due to

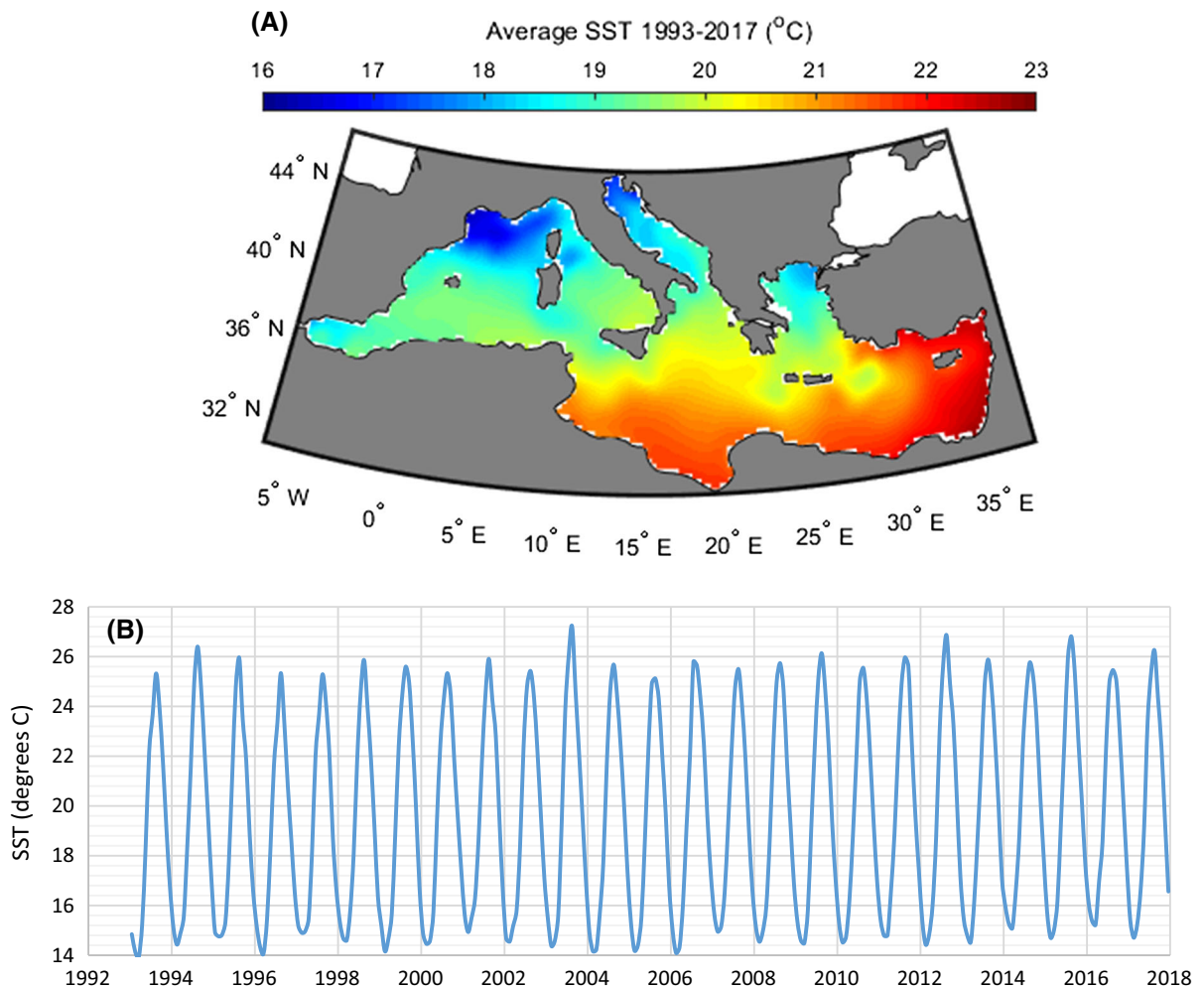


Figure 10

Statistics of the AVHRR-derived SST monthly dataset from a 25-year period (1993–2017): **a** spatial distribution of temporal mean, **b** time variation of spatial mean

the Mid-Ionian Jet was reinforced by the Ionian cyclonic circulation (Gačić et al. 2014). The third SLA mode (3.9% of the total de-seasoned variance) indicates a spatial maximum in the north of the Ionian Sea.

The first three EOF modes of SSTA explain about 68.1% of the total deseasoned variance of the data as shown in Fig. 13. The first mode is explaining 40.7% of the total deseasoned variance. The spatial pattern has shown positive values throughout the whole Mediterranean Sea, indicating an in-phase oscillation of the whole basin around the steady-state mean. The highest SSTA variability was observed over the

central part of the Mediterranean Sea with maximum amplitude in the Tyrrhenian Sea. Meanwhile, the minimum variability of SSTA was found in the western and eastern part of the Mediterranean Sea with minimum amplitude in the Alboran and Aegean Seas. This minimum variability is due to two reasons: the first one is the presence of strong and persistent winds like Tramontane and Mistral on the northwestern Mediterranean and the Etesian winds in the Levantine basin (Pastor et al. 2017); the second reason is the input of external water masses, such as the Atlantic cold-water inflow through the Gibraltar Strait into the Alboran Sea, and the Black Sea cold-

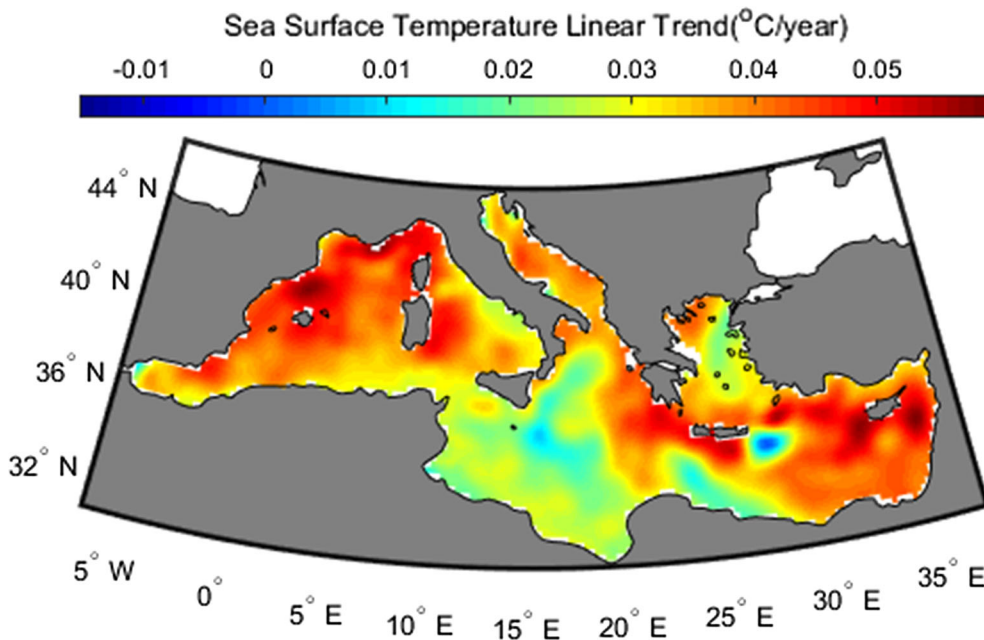


Figure 11

Map of the Mediterranean SST trends (linear variation with time) from AVHRR during 1993–2017

water inflow through the Dardanelles Strait into the Aegean Sea (Skirris et al. 2011). From the corresponding PC1 time series, the highest positive peak of inter-annual variability was found in summer 2003, which was the warmest summer during our record period. The highest negative peak was observed in the winter of 1996, which was the coldest winter during the period of investigation. These results are in good agreement with Skirris et al. (2012).

The second mode of SSTA explains about 21.3% of the total deseasoned variance of the data. The spatial distribution is a dipole, which shows opposite variation between the eastern and western sub-basins. In the western basin, the maximum variability was found offshore the Gulf of Lions, while the maximum variability with opposite sign was observed in the Levantine and the Aegean basins. In summary, the corresponding PC2 time series shows an alternation of positive and negative trends during the period of 1993–2017. The third SSTA mode explains about 6.1% of the total de-seasoned variance. The spatial distribution of this mode shows an out-of-phase

oscillation of the central and western/eastern parts of the Mediterranean Sea.

3.7. Effect of SST on Sea Level and Correlation Map

The coupled variability of the sea level and SST is investigated by computing a simple Pearson correlation of the time-series at the same spatial points. The Pearson correlation corresponding to different time-lags is evaluated. The correlation analysis shows that the SLA and SSTA are strongly correlated at seasonal scales in the whole Mediterranean Sea, except over the Adriatic Sea. The highest correlation ($R = 0.61$) was observed over the western Mediterranean Sea. This indicates that the SST significantly affects the observed Mediterranean Sea level except over the Adriatic Sea. The highest correlation between SSTA and SLA is obtained throughout the Mediterranean Sea ($R = 0.83$) after the latter has been delayed by 2 months compared to SSTA. The delay results from the downward propagation of heat in the upper ocean layers (Fenoglio-Marc 2002).

Figure 14 reports that after the seasonal cycle has been removed, the spatial correlation between SLA

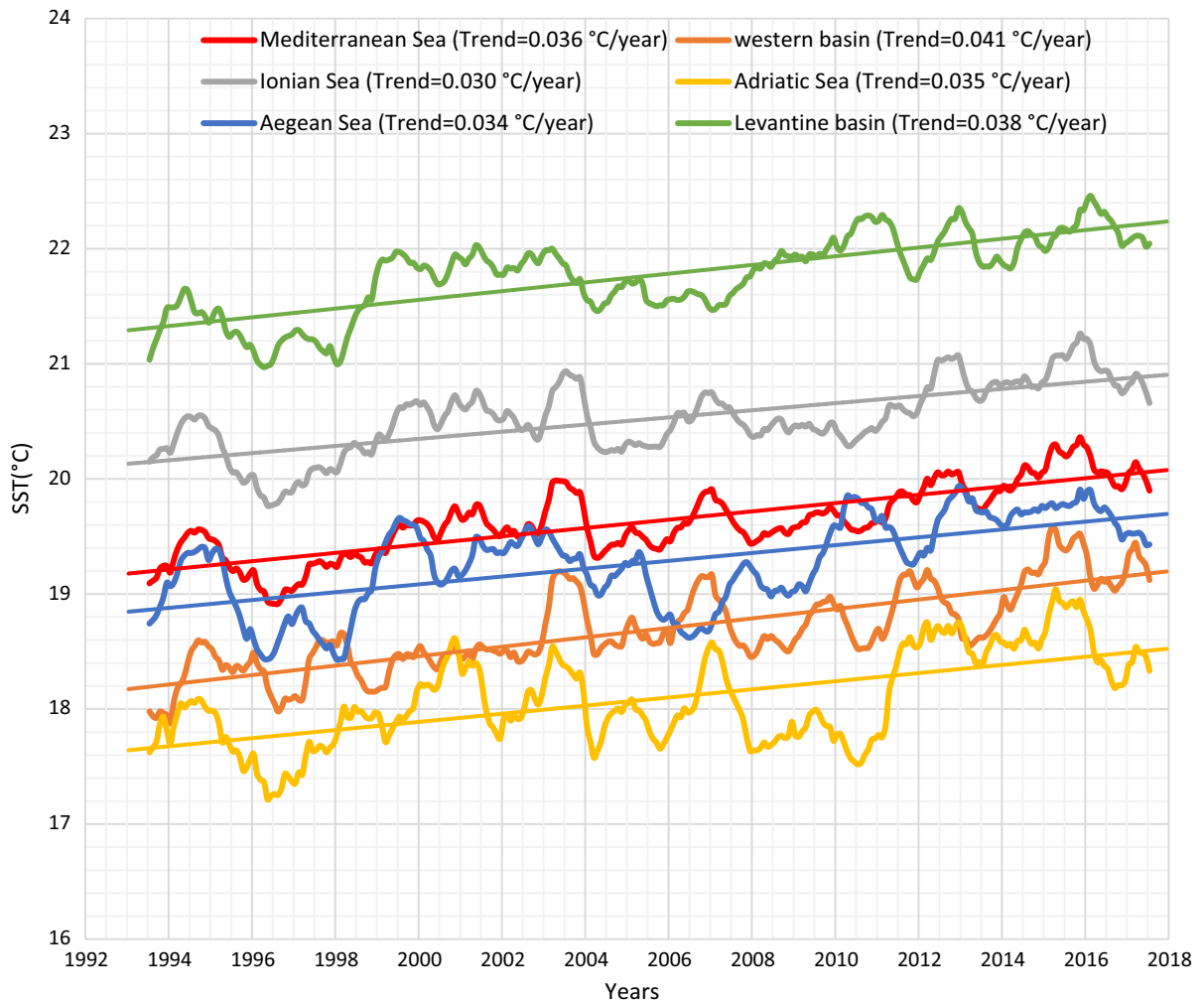


Figure 12

The deseasoned sea surface temperature time-series and linear trends for Mediterranean Sea and its sub-basins

and SSTA decreases significantly over the whole basin, except in the Aegean and Levantine basins (correlation up to 0.6). In the eastern part, inter-annual variability is higher than in the western Mediterranean, where the seasonal cycle dominates (Fenoglio-Marc 2002). Since SST is an indicator of thermosteric variations, the high correlation between SLA and SSTA in the Aegean and Levantine basins implies that the inter-annual linear sea level trend has been largely driven by thermosteric effects. Comparing the linear trend in sea level and sea surface temperature (Figs. 3 and 11), we see a general

increase in sea level in the Mediterranean Sea, where the SST rose in general, and a drop in sea level in the Ionian Sea and Ierapetra gyre, where the SST dropped (with the exception of the western Mediterranean). In view of the high spatial correlation between SLA and SST linear trends in the Eastern Mediterranean, the SST trend suggests an increase in the thermosteric effect, which appears to be the main factor that controls the sea level trend.

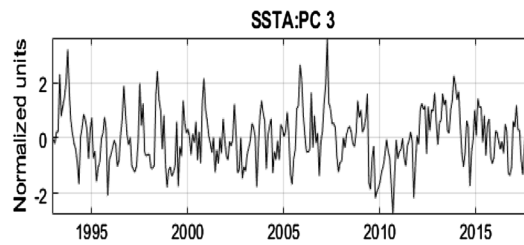
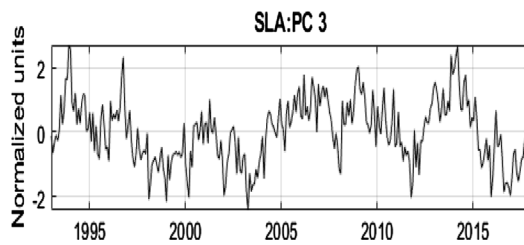
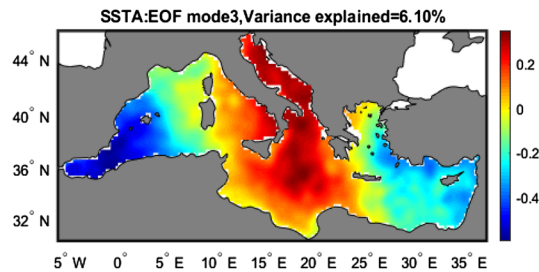
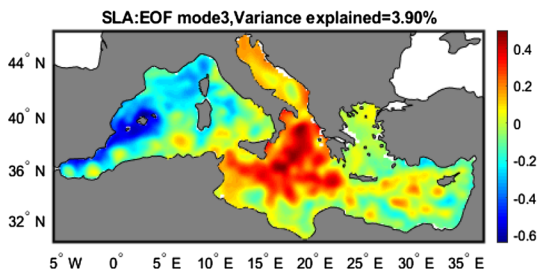
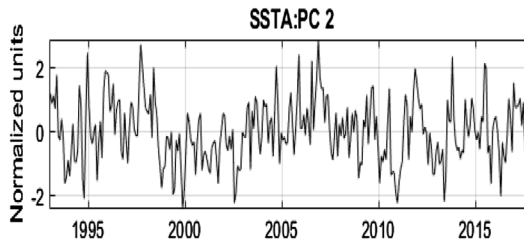
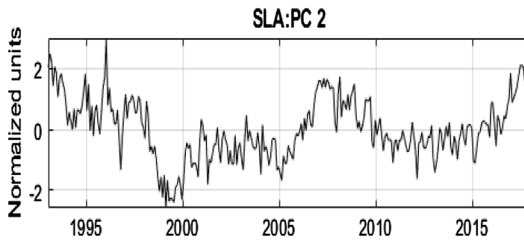
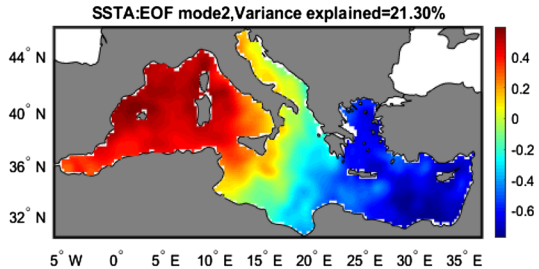
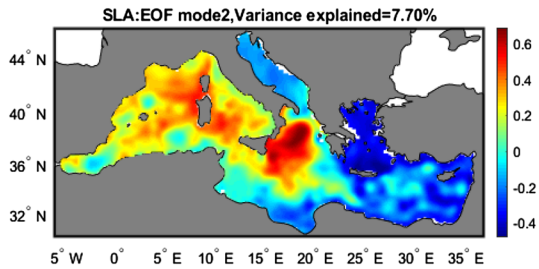
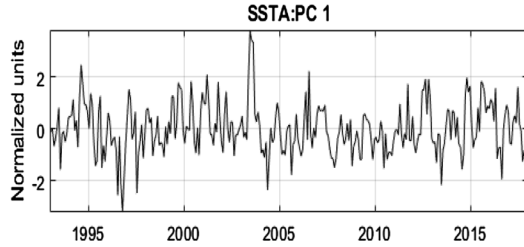
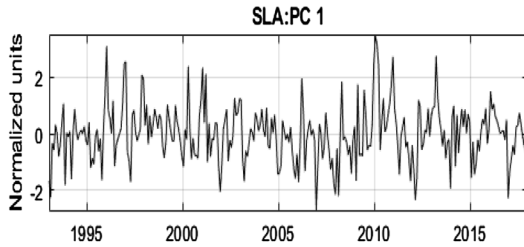
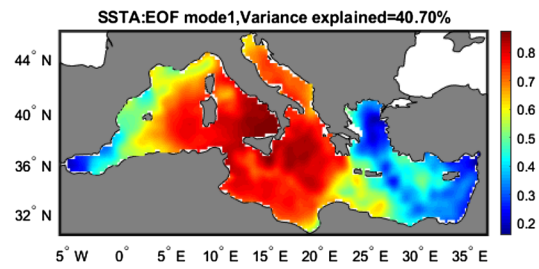
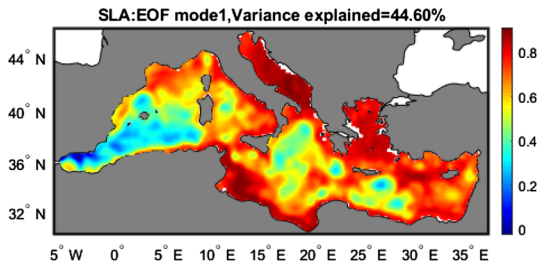


Figure 13

The first three EOF/PC (spatial variation/temporal variation) modes of the inter-annual variability for SLA (left) and SSTA (right) in the Mediterranean Sea during 1993–2017 (trend and seasonal cycles have been removed)

4. Summary and Conclusions

This paper has provided a comprehensive and up-to-date assessment of sea level changes in the Mediterranean Sea and its relation to sea surface temperature, using altimetry and TG data during the 25-year period from January 1993 to December 2017. The study has investigated inter-annual variability and long-term trends. The conclusions are summarized as follows:

The average absolute sea level trend in Mediterranean Sea from satellite altimetry during the period 1993–2017 was 2.5 ± 0.41 mm/year. After the GIA correction, the basin average trend was 2.7 ± 0.41 mm/year, a value which is not statistically different from the global average rate of 3.19 ± 0.63 mm/year estimated by Chambers et al. (2017) during the period 1993–2015. However, there was considerable spatial variability in the trends

across the study area, ranging from -5.6 to 5.3 mm/year. The highest trends were found in the Aegean, Adriatic, and Levantine basins.

Positive trends were observed for the period 1993–2017 for all available tide gauge records. The longest tide gauge time series (more than 130 years) at Marseille and Trieste showed trends of 1.17 ± 0.03 and 1.09 ± 0.04 mm/year, respectively, which are insignificantly different from the global mean sea level rise for the twentieth century. By contrast, two stations (Levkas in Greece and Antalya II in Turkey), have a large trend (more than 6 mm/year) significantly influenced by local vertical land motions. The atmospheric pressure contribution at tide gauges accounts for 12–36% of the observed sea level variability and shows positive trends between 0 and 0.96 mm/year, this result is in good agreement with Gomis et al. (2008), as they showed that the situation was drastically different during the last decade and the trend of the contribution of atmospheric pressure calculated for the period 1993–2001 was positive. The modelled GIA effect in tide gauges ranges between -0.17 and 0.3 mm/year.

The sea level signal from both altimetry and tide gauges revealed extremely large fluctuations in the

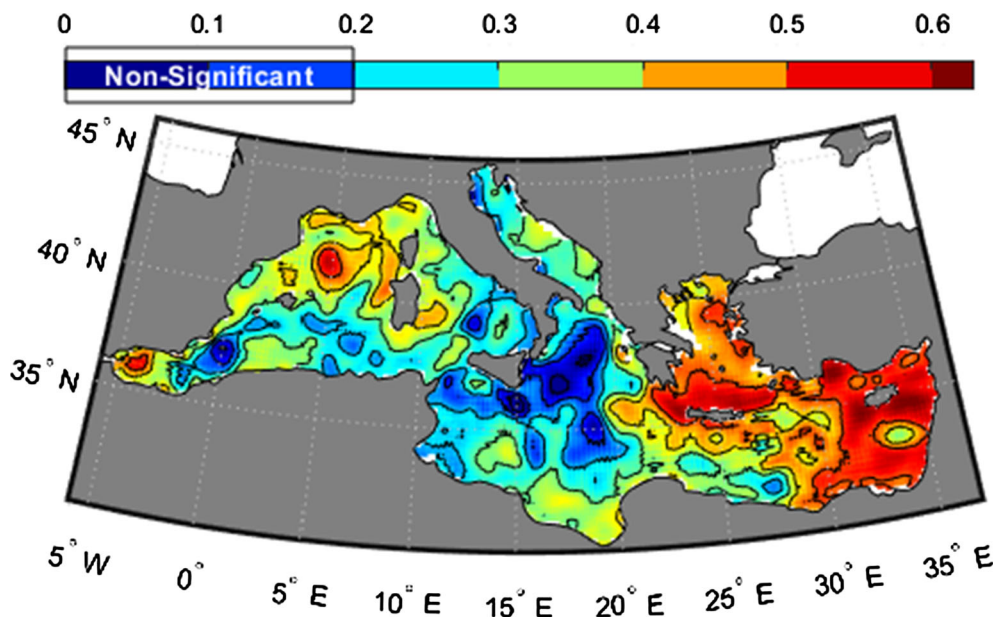


Figure 14

Monthly Pearson correlation map between SLA and SSTA during 1993–2017. Results after removing of seasonal cycle

extended winters (December–March) of 2009–2010 and 2010–2011, which occurred throughout a strong negative phase of the NAO index, in agreement with Landerer and Volkov (2013). This event was characterized by a non-steric fluctuations, because of mass transport through the Strait of Gibraltar is mainly driven by wind according to Tsimplis et al. (2013). Overall, we note that from all TG stations and from altimetry for different sub-basins, there were large negative sea level anomalies in the extended winter of 2011–2012, which is highly correlated to the strong positive phase of NAO Index (see Fig. 6).

Analysis of sea surface temperature (SST) data for the same time span indicated that the warming rate was about 0.036 ± 0.003 °C/year over the whole Mediterranean Sea, supporting previous findings reported in Pastor et al. (2017). The correlation analysis shows that the SLA and SSTA are strongly correlated at seasonal scales in the whole Mediterranean Sea, except over the Adriatic Sea. After the seasonal cycle has been removed from both time series, the correlations are strongly decreasing over the whole basin, except in the Aegean and Levantine Basins. The comparison between sea level and SST linear trend maps (see Figs. 3 and 11) showed that both sea level and SST are either increasing (or decreasing) simultaneously in the eastern Mediterranean. These suggests that the thermosteric effect, can have a strong influence on sea level change in the eastern Mediterranean Sea.

The inter-annual spatiotemporal variability of SLA and SSTA was estimated using EOF/PC analysis. The spatial EOF pattern of the first mode of sea level and SST showed an in-phase oscillation of the whole Mediterranean Sea. This can indicate an in-phase heating or cooling (addition or loss) of the whole Mediterranean water volume. The highest spatial variability of SLA was observed over the Adriatic and Aegean Seas, most of the Levantine basin, and along the Tunisian shelf. The highest SSTA variability was observed over the central part of the Mediterranean Sea with maximum amplitude in the Tyrrhenian Sea. From the corresponding principal component time series, the highest temporal variability of sea level and SST was found in 2010 and 2003, respectively.

The second SLA mode revealed an out-of-phase variability of the North Ionian Gyre and the Aegean/Levantine Basins sea level. The corresponding time series has shown a decadal variability, due to the decadal inversions of the Ionian surface layer (Gačić et al. 2011). The second SST mode exhibits a spatial dipole indicating opposite variation between the eastern and western sub-basins. The corresponding time series shows an alternation of positive and negative trends during the period of study. The first EOF mode of both SLA and SST showed an in-phase oscillation over the entire Mediterranean Sea, while the second mode showed that they are in-phase only in the Aegean and Levantine Basins. This can largely explain the higher effect of SST on the sea level in the Aegean and Levantine Basins.

Acknowledgements

Authors would like to acknowledge the organizations that provided the sources of the data used in this work, including CMEMS Project for the altimetry products, the Permanent Service for Mean Sea Level (PSMSL) for tide gauge data, NOAA for the SST&NAO data, and ECMWF for providing a comprehensive access to SLP data. We would like to thank Prof. Nikolaos Skliris (University of Southampton) for his constructive and helpful comments on the revised manuscript. The authors are also grateful to the anonymous reviewers, who have greatly improved the quality of this work with their advice and helpful remarks.

Publisher's Note Springer Nature remains neutral with regard to jurisdictional claims in published maps and institutional affiliations.

REFERENCES

- Belkin, I. M. (2009). Rapid warming of large marine ecosystems. *Progress in Oceanography*. <https://doi.org/10.1016/j.pocean.2009.04.011>.
- Bonaduce, A., Pinaridi, N., Oddo, P., Spada, G., & Larnicol, G. (2016). Sea-level variability in the Mediterranean Sea from altimetry and tide gauges. *Climate Dynamics*, 47(9–10), 2851–2866.

- Calafat, F. M., Chambers, D. P., & Tsimplis, M. N. (2012). Mechanisms of decadal sea level variability in the eastern North Atlantic and the Mediterranean Sea. *Journal of Geophysical Research: Oceans*. <https://doi.org/10.1029/2012JC008285>.
- Calafat, F. M., & Gomis, D. (2009). Reconstruction of Mediterranean sea level fields for the period 1945–2000. *Global and Planetary Change*. <https://doi.org/10.1016/j.gloplacha.2008.12.015>.
- Carrère, L., & Lyard, F. (2003). Modeling the barotropic response of the global ocean to atmospheric wind and pressure forcing - Comparisons with observations. *Geophysical Research Letters*. <https://doi.org/10.1029/2002GL016473>.
- Cazenave, A., Bonnefond, P., Mercier, F., Dominh, K., & Toumazou, V. (2002). Sea level variations in the Mediterranean Sea and Black Sea from satellite altimetry and tide gauges. *Global and Planetary Change*. [https://doi.org/10.1016/S0921-8181\(02\)00106-6](https://doi.org/10.1016/S0921-8181(02)00106-6).
- Cazenave, A., Cabanes, C., Dominh, K., & Mangiarotti, S. (2001). Recent sea level change in the Mediterranean sea revealed by Topex/Poseidon satellite altimetry. *Geophysical Research Letters*, 28(8), 1607–1610. <https://doi.org/10.1029/2000GL012628>.
- Chambers, D. P., Cazenave, A., Champollion, N., Dieng, H., Llovel, W., Forsberg, R., et al. (2017). Evaluation of the global mean sea level budget between 1993 and 2014. *Surveys in Geophysics*, 38(1), 309–327.
- Church, J. A., Clark, P. U., Cazenave, A., Gregory, J. M., Jevrejeva, S., Levermann, A., et al. (2013). *Sea level change. Climate change 2013: The physical science basis. Contribution of working group I to the fifth assessment report of the intergovernmental panel on climate change*, 1137–1216. <https://doi.org/10.1017/CBO9781107415315.026>.
- Church, J. A., Gregory, J., Huybrechts, P., Kuhn, M., Lambeck, K., Nhuan, M., et al. (2001). *Changes in sea level. Climate change 2001: The scientific basis: Contribution of working group I to the third assessment report of the intergovernmental panel*, 639–694. <http://epic.awi.de/4506/1/Chu2001a.pdf%5Cnpapers://f554698c-bc30-43aa-8c0c-c8de8adb48e4/Paper/p2603>.
- Church, J. A., & White, N. J. (2011). Sea-level rise from the late 19th to the early 21st century. *Surveys in Geophysics*, 32(4–5), 585–602.
- Criado-Aldeanueva, F., Vera, J. D. R., & García-Lafuente, J. (2008). Steric and mass-induced Mediterranean Sea level trends from 14 years of altimetry data. *Global and Planetary Change*, 60(3), 563–575.
- Dasgupta, S., Laplante, B., Murray, S., & Wheeler, D. (2011). Exposure of developing countries to sea-level rise and storm surges. *Climatic Change*, 106(4), 567–579.
- Dee, D. P., Uppala, S. M., Simmons, A. J., Berrisford, P., Poli, P., Kobayashi, S., et al. (2011). The ERA-Interim reanalysis: Configuration and performance of the data assimilation system. *Quarterly Journal of the Royal Meteorological Society*, 137(656), 553–597.
- Ducet, N., Le Traon, P. Y., & Reverdin, G. (2000). Global high-resolution mapping of ocean circulation from TOPEX/Poseidon and ERS-1 and-2. *Journal of Geophysical Research: Oceans*, 105(C8), 19477–19498.
- Emery, W. J., & Thomson, R. E. (1998). Data Analysis Methods in Physical Oceanography. *Estuaries*, 22(December), 638. <https://doi.org/10.2307/1353059>.
- Fenoglio-Marc, L. (2002). Long-term sea level change in the Mediterranean Sea from multi-satellite altimetry and tide gauges. *Physics and Chemistry of the Earth, Parts A/B/C*, 27(32), 1419–1431.
- Gačić, M., Civitarese, G., Eusebi Borzelli, G. L., Kovačević, V., Poulain, P. M., Theocharis, A., et al. (2011). On the relationship between the decadal oscillations of the northern Ionian Sea and the salinity distributions in the eastern Mediterranean. *Journal of Geophysical Research: Oceans*. <https://doi.org/10.1029/2011JC007280>.
- Gačić, M., Civitarese, G., Kovacevic, V., Ursella, L., Bensi, M., Menna, M., et al. (2014). Extreme winter 2012 in the Adriatic: An example of climatic effect on the BiOS rhythm. *Ocean Science*, 10(3), 513.
- Gačić, M., Eusebi Borzelli, G. L., Civitarese, G., Cardin, V., & Yari, S. (2010). Can internal processes sustain reversals of the ocean upper circulation? The Ionian Sea example. *Geophysical Research Letters*. <https://doi.org/10.1029/2010GL043216>.
- Gaspar, P., & Ponte, R. M. (1997). Relation between sea level and barometric pressure determined from altimeter data and model simulations. *Journal of Geophysical Research: Oceans*, 102(C1), 961–971.
- Gomis, D., Ruiz, S., Sotillo, M. G., Álvarez-Fanjul, E., & Terradas, J. (2008). Low frequency Mediterranean sea level variability: The contribution of atmospheric pressure and wind. *Global and Planetary Change*. <https://doi.org/10.1016/j.gloplacha.2008.06.005>.
- Haddad, M., Hassani, H., & Taibi, H. (2013). Sea level in the Mediterranean Sea: Seasonal adjustment and trend extraction within the framework of SSA. *Earth Science Informatics*, 6(2), 99–111.
- Holgate, S. J., Matthews, A., Woodworth, P. L., Rickards, L. J., Tamsiea, M. E., Bradshaw, E., et al. (2013). New data systems and products at the permanent service for mean sea level. *Journal of Coastal Research*, 288, 493–504. <https://doi.org/10.2112/JCOASTRES-D-12-00175.1>.
- Landerer, F. W., & Volkov, D. L. (2013). The anatomy of recent large sea level fluctuations in the Mediterranean Sea. *Geophysical Research Letters*, 40(3), 553–557.
- Maiyya, I. A., & El-Geziry, T. M. (2012). Long term sea-level variation in the south-eastern Mediterranean Sea: A new approach of examination. *Journal of Operational Oceanography*, 5(2), 53–59.
- Marcos, M., & Tsimplis, M. N. (2008). Coastal sea level trends in Southern Europe. *Geophysical Journal International*. <https://doi.org/10.1111/j.1365-246X.2008.03892.x>.
- Marullo, S., Santoleri, R., Ciani, D., Le Borgne, P., Péré, S., Pinardi, N., et al. (2014). Combining model and geostationary satellite data to reconstruct hourly SST field over the Mediterranean Sea. *Remote Sensing of Environment*, 146, 11–23.
- Mertz, F., Rosmorduc, V., Maheu, C., & Faugère, Y. (2017). Product user manual for sea level SLA products. *Copernicus Marine Environment Monitoring Service*. <http://marine.copernicus.eu/documents/PUM/CMEMS-SL-PUM-008-032-051.pdf>. Accessed 10 Nov 2018.
- Nykjaer, L. (2009). Mediterranean Sea surface warming 1985–2006. *Climate Research*, 39(1), 11–17.
- Overland, J. E., & Preisendorfer, R. W. (1982). A significance test for principal components applied to a cyclone climatology. *Monthly Weather Review*, 110(1), 1–4.
- Pastor, F., Valiente, J. A., & Palau, J. L. (2017). Sea surface temperature in the mediterranean: Trends and spatial patterns (1982–2016). *Pure and Applied Geophysics*. <https://doi.org/10.1007/s00024-017-1739-z>.

- Peltier, W. R., Argus, D. F., & Drummond, R. (2015). Space geodesy constrains ice age terminal deglaciation: The global ICE-6G_C (VM5a) model. *Journal of Geophysical Research: Solid Earth*, *120*(1), 450–487.
- Pinardi, N., Zavatarelli, M., Adani, M., Coppini, G., Fratianni, C., Oddo, P., et al. (2015). Mediterranean Sea large-scale low-frequency ocean variability and water mass formation rates from 1987 to 2007: A retrospective analysis. *Progress in Oceanography*, *132*, 318–332.
- Preisendorfer, R. W., & Mobley, C. D. (1988). *Principal component analysis in meteorology and oceanography* (Vol. 425). Amsterdam: Elsevier.
- Reynolds, R. W., Smith, T. M., Liu, C., Chelton, D. B., Casey, K. S., & Schlax, M. G. (2007). Daily high-resolution-blended analyses for sea surface temperature. *Journal of Climate*, *20*(22), 5473–5496.
- Rio, M. H., Pascual, A., Poulain, P. M., Menna, M., Barceló, B., & Tintoré, J. (2014). Computation of a new mean dynamic topography for the Mediterranean Sea from model outputs, altimeter measurements and oceanographic in situ data. *Ocean Science*, *10*(4), 73.
- Rio, M. H., Poulain, P. M., Pascual, A., Mauri, E., Larnicol, G., & Santoleri, R. (2007). A mean dynamic topography of the Mediterranean Sea computed from altimetric data, in situ measurements and a general circulation model. *Journal of Marine Systems*, *65*(1), 484–508.
- Rixen, M., Beckers, J. M., Levitus, S., Antonov, J., Boyer, T., Maillard, C., et al. (2005). The western mediterranean deep water: A proxy for climate change. *Geophysical Research Letters*. <https://doi.org/10.1029/2005GL022702>.
- Shaltout, M., & Omstedt, A. (2014). Recent dynamic topography changes in the Mediterranean Sea analysed from satellite altimetry data. *Current Development in Oceanography*, *7*(1/2), 1.
- Skliris, N., Sofianos, S. S., Gkanasos, A., Axaopoulos, P., Mantziafou, A., & Vervatis, V. (2011). Long-term sea surface temperature variability in the Aegean Sea. *Advances in Oceanography and Limnology*. <https://doi.org/10.1080/19475721.2011.601325>.
- Skliris, N., Sofianos, S., Gkanasos, A., Mantziafou, A., Vervatis, V., Axaopoulos, P., et al. (2012). Decadal scale variability of sea surface temperature in the Mediterranean Sea in relation to atmospheric variability. *Ocean Dynamics*, *62*(1), 13–30.
- Stammer, D., Cazenave, A., Ponte, R. M., & Tamisiea, M. E. (2013). Causes for contemporary regional sea level changes. *Annual Review of Marine Science*, *5*, 21–46.
- Stanev, E. V., Le Traon, P. Y., & Peneva, E. L. (2000). Sea level variations and their dependency on meteorological and hydrological forcing: Analysis of altimeter and surface data for the Black Sea. *Journal of Geophysical Research-Oceans*, *105*(C7), 17203–17216.
- Tsimplis, M. N., Calafat, F. M., Marcos, M., Jordà, G., Gomis, D., Fenoglio-Marc, L., et al. (2013). The effect of the NAO on sea level and on mass changes in the Mediterranean Sea. *Journal of Geophysical Research: Oceans*. <https://doi.org/10.1002/jgrc.20078>.
- Tsimplis, M. N., & Rixen, M. (2002). Sea level in the Mediterranean Sea: the contribution of temperature and salinity changes. *Geophysical Research Letters*, *29*(23), 51–1. <https://doi.org/10.1029/2002gl015870>.
- Tsimplis, M., Spada, G., Marcos, M., & Flemming, N. (2011). Multi-decadal sea level trends and land movements in the Mediterranean Sea with estimates of factors perturbing tide gauge data and cumulative uncertainties. *Global and Planetary Change*, *76*(1–2), 63–76.
- Vera, J. D. R., Criado-Aldeanueva, F., García-Lafuente, J., & Soto-Navarro, F. J. (2009). A new insight on the decreasing sea level trend over the Ionian basin in the last decades. *Global and Planetary Change*, *68*(3), 232–235.
- Vigo, I., Garcia, D., & Chao, B. F. (2005). Change of sea level trend in the Mediterranean and Black seas. *Journal of Marine Research*. <https://doi.org/10.1357/002224005775247607>.
- Vigo, M. I., Sánchez-Reales, J. M., Trottini, M., & Chao, B. F. (2011). Mediterranean Sea level variations: Analysis of the satellite altimetric data, 1992–2008. *Journal of Geodynamics*, *52*(3), 271–278.
- von Storch, H., & Zwiers, F. W. (1999). *Statistical analysis in climate research* (p. 484). Cambridge: Cambridge University Press.
- Woodworth, P. L., & Player, R. (2003). The permanent service for mean sea level: An update to the 21st century. *Journal of Coastal Research*. <https://doi.org/10.2112/JCOASTRES-D-12-00>.
- Zerbini, S., Plag, H. P., Baker, T., Becker, M., Billiris, H., Bürki, B., et al. (1996). Sea level in the Mediterranean: A first step towards separating crustal movements and absolute sea-level variations. *Global and Planetary Change*, *14*(1–2), 1–48.

(Received July 23, 2018, revised February 20, 2019, accepted March 8, 2019, Published online March 27, 2019)